To The Graduate Council

I am submitting herewith a thesis written by Yuanheng Zhang entitled "Process to Create PP/Fiber Glass Composite for Reinforcing Portland Cement Products." I have examined the final copy of this thesis for form and content and recommend that it be accepted in partial fulfillment of the requirements for the degree of Master of Science, with a major in Polymer Engineering

John F. Fellers

John F Fellers, Major Professor

We have read this thesis
and recommend its acceptance:

Accepted for the Council:

Associate Vice Chancellor and
Dean of The Graduate School

Process to Create PP/Fiber Glass Composite for Reinforcing Portland Cement Products

A Thesis Presented for the Master of Science Degree
The University of Tennessee, Knoxville

Yuanheng Zhang

December, 2000

DEDICATION

This thesis is dedicated to my wife, Gao Xiao, and my parents, Zhang shıxiang, Ji ronghua, my uncle, Zhang Shihua They give me so much courage, support, endless love and so many invaluable educatıonal opportunıties

ACKNOWLEDGEMENTS

I am very glad to have had the opportunity to come to The University of Tennessee to study from People's Republic of China. Although there were some initial difficulties for me as a foreign student at first, many people offered me support and made my stay most enjoyable. The memories are precious.

I would like to thank the members of my Advisory Committee, Dr. Joseph Spruiell and Dr Roberto Benson, for their time and expertise. I would like to particularly thank my major professor - Dr John F. Fellers for his support, kindness, and guidance. He was always very nice and patient with me, and gave me many valuable suggestions. During the three years of study, I learned not only technical knowledge, but also learned how to be a better person with a valuable perspective on life. Lastly, I would like to thank all the people who gave me help during my study in the University of Tennessee.

ABSTRACT

This work explores and studies the uninterrupted filament winding process for fabricating structures made of polypropylene and glass fiber. Based on this work, a unique fuzzy inner surface of tubes and the key role of the mandrel temperature on the composite's mechanical properties were observed. It was concluded that the fuzzy inner surface of the tube can improve the strength and fatigue property of the composite and the higher mandrel temperature can diminish the void content within the composite and improve the mechanical properties of the composite. Steel rebar, thermoset pipe and rebar produced by filament winding or pultrusion have long been used for reinforcing cement, but these products suffer from corrosion, high cost and poor toughness. Through greatly improving the resin's wetting ability to glass fiber bundle, and more precise control of the process elements, this project starts as a way to produce composite tube made from polypropylene and glass fiber that offers some improved properties, while being cheaper and tougher. The tubes were filled with a cement mixture and some of them were reinforced with internal tapes. Three point bending experiments, microscope observation, and image analysis were used as the investigative tools in this work. Processing elements such as the mandrel temperature, wetting die temperature, wetting die rotating speed, exit gate pressure etc., were studied and the relationship between the processing elements and the mechanical properties was investigated.

TABLE OF CONTENTS

CHAPTER **PAGE**

I INTRODUCTION **1**

II LITERATURE REVIEW **3**

PORTLAND CEMENT AND STEEL CONCRETE 3

CORROSION OF STEEL IN CONCRETE 6

FIBER REINFORCED PLASTICS FOR REINFORCING CONCRETE 9

The FRP Reinforcing Bars *10*

Fiber Reinforced Plastic Grid *15*

Fiber Reinforced Plastic Plate *16*

Hollow fiber reinforced plastic composite column *17*

Concrete column reinforced with fiber reinforced plastic strap wrapping *18*

GLASS FIBER REINFORCED CONCRETE 19

THERMOPLASTIC COMPOSITES 20

INTERFACES AND INTERPHASES IN THERMOPLASTIC COMPOSITES 24

THE IN-SITU THERMOPLASTIC FILAMENT WINDING PROCESS 26

III EXPERIMENTAL **32**

OBJECTIVE 32

MATERIALS 32

PROCESSING EQUIPMENT 34

ROUTINE OF PROCESSING AND TESTING METHODS 37

Processing procedure of the hollow composite column *37*

Reinforcing the cement mixture with tube *39*

Three points bending tests *39*

Sample polishing and microscopic observation *40*

Nonuniformity analysis of glass fiber distribution *40*

The study for void amount within Sample's cross-section 42

Fatigue test 42

IV RESULT AND DISCUSSION **44**

THE EFFECT OF MANDREL TEMPERATURE 44

Inner surface of tubes made using different mandrel temperatures . 45

Mechanical properties . 46

The Elastic modulus 51

The Absorbed Energy 53

The microscopic observation . 53

The glass fiber's distribution within the polypropylene matrix 55

THE EFFECT OF WETTING DIE TEMPERATURE 58

THE EFFECT OF EXIT GATE PRESSURE 58

THE EFFECT OF THE USAGE OF THE PRE-OPEN DEVICE 61

THE EFFECT OF THE WETTING DIE'S ROTATING SPEED 62

THE REINFORCEMENT OF CEMENT FILLED TUBE BY INTERNALLY PLACED PP/FIBERGLASS TAPE 64

THE FATIGUE TEST 66

CONCLUSIONS **68**

BIBLIOGRAPHY **70**

VITA **76**

LIST OF TABLES

TABLE 2-1. AVERAGE PHYSICAL PROPERTIES OF BUILDING STONE, BRICK AND CONCRETE . 4

TABLE 2-2 MECHANICAL PROPERTIES OF STEEL 5

TABLE 2-3. THERMOPLASTICS VERSUS THERMOSETS 22

TABLE 3-1. THE GLASS FIBER'S PHYSICAL PROPERTIES 33

TABLE 3-2 POLYPROPYLENE'S PHYSICAL PROPERTIES 34

TABLE 4-1 EXPERIMENTAL PLAN FOR THE STUDY OF MANDREL TEMPERATURE EFFECT ON MECHANICAL PROPERTIES OF THE TUBE FILLED WITH CEMENT 45

TABLE 4-2 THE DISPLACEMENTS OF DIFFERENT TUBE FILLED WITH CEMENT MADE UNDER DIFFERENT MANDREL TEMPERATURE 49

TABLE 4-3 THE STUDY FOR WETTING DIE TEMPERATURE'S EFFECT ON MECHANICAL PROPERITY OF THE TUBE FILLED WITH CEMENT 58

TABLE 4-4 THE STUDY OF EXIT GATE PRESSURE EFFECT ON MECHANICAL PROPERTY OF THE TUBE FILLED WITH CEMENT 60

TABLE 4-5 THE STUDY FOR EFFECT OF THE USAGE OF THE PRE-OPEN DEVICE ON MECHANICAL PROPERTIES OF THE TUBE FILLED WITH CEMENT 61

TABLE 4-6 THE STUDY FOR EFFECT OF DIFFERENT WETTING DIE SPEED ON MECHANICAL PROPERTIES OF THE TUBE FILLED WITH CEMENT 62

TABLE 4-7. THE PROCESSING FACTORS OF THE TUBE USED OF INTERNAL TAPE REINFORCED 64

TABLE 4-8. THE MECHANICAL PROPERTY OF THE TUBE REINFORCED WITH INTERNALLY TAPES 65

TABLE 4-9. THE PROCESSING FACTORS USED TO MAKE TUBES TO BE REINFORCED WITH INTERNAL TAPES 66

LIST OF FIGURES

FIGURE 2-1. FRP REINFORCEMENT TYPES 9
FIGURE 2-2 THREE-DIMENSIONAL FRP GRID AND FIBER WRAPPING 10
FIGURE 2-3 FABRICATION OF FRP REINFORCING BAR 11
FIGURE 2-4 THE SKETCH OF HOOKED GLASS FIBER REINFORCED PLASTIC 13
FIGURE 2-5 FRP-CONCRETE COMPOSITE COLUMN 17
FIGURE 2-6 GENERAL BLOCK DIAGRAM OF SAYRE'S EXPERIMENTAL SETUP 30
FIGURE 3-1. PROCESSING FACTORS 33
FIGURE 3-2 GENERAL BLOCK DIAGRAM OF EXPERIMENTAL SETUP 35
FIGURE3-3. A PHOTOGRAPH OF THE COMPLETE WINDING FACILITY 36
FIGURE 3-4 A CLOSE-UP OF THE PRE-OPEN DEVICE, WETTING DIE AND THE MANDREL 36
FIGURE3-5. THE DIAGRAM PROCESSING PROCEDURE OF THE HOLLOW COMPOSITE TUBES 38
FIGURE 3-7. AN EXAMPLE OF HOW THE ¼ PHOTO WAS SPLIT IN TO 8×8 PIECES 41
FIGURE 3-8. THE VOID AREA SELECTED BY THE "THRESHOLD TOOL" 43
FIGURE 3-9 THRESHOLD DIALOGUE BOX WHICH SHOWS THE FIGURE 3-8 HAS 8 07% VOIDS 43
FIGURE 4-1. DIFFERENT INNER SURFACE APPEARANCE OF THE TUBES MADE UNDER DIFFERENT MANDREL TEMPERATURE 47
FIGURE 4-2 THE THREE POINT BENDING TEST FOR THE CEMENT FILLED CYLINDER PRODUCED WITH FOUR DIFFERENT MANDREL TEMPERATURES 48
FIGURE 4-3 THE FRACTURE SURFACE OF THE TUBE FILLED WITH CEMENT MADE AT DIFFERENT MANDREL TEMPERATURES 50
FIGURE 4-4 THE SIDE-VIEW OF THE FRACTURE SURFACE OF THE TUBE MADE AT MANDREL TEMPERATURE 165°C 51
FIGURE 4-5 ELASTIC MODULUS OF THE TUBE FILLED WITH CEMENT MADE UNDER DIFFERENT MANDREL TEMPERATURES 52
FIGURE 4-6 THE ABSORBED ENERGY OF THE CEMENT MIXTURE FILLED TUBES MADE AT DIFFERENT MANDREL TEMPERATURES 54
FIGURE 4-7 CROSS-SECTION OF THE TUBE PROCESSED AT HIGH TEMPERATURE 54

FIGURE 4-8. MICROSCOPIC PHOTO OF A CROSS-SECTION OF A 140°C (50×) 56
FIGURE 4-9 MICROSCOPIC PHOTO OF A CROSS-SECTION OF A 145°C (50×).. 56
FIGURE 4-10. MICROSCOPIC PHOTO OF A CROSS-SECTION OF A 155°C (50×)..... 56
FIGURE 4-11 MICROSCOPIC PHOTO OF A CROSS-SECTION OF A 165°C (50×). 56
FIGURE 4-12 THE PERCENTAGE OF VOID IN THE TUBES' CROSS-SECTION MADE UNDER DIFFERENT TEMPERATURES 57
FIGURE 4-13 COEFFICIENT OF VARIATION SPECTRA OF GLASS FIBER DISTRIBUTION OF THE TUBES MADE UNDER DIFFERENT MANDREL TEMPERATURES 57
FIGURE 4-14 THE LOAD VS DISPLACEMENT FOR TWO TUBES FILLED WITH CEMENT MADE UNDER TWO DIFFERENT WETTING DIE TEMPERATURES. 59
FIGURE 4-15 THE ABSORBED ENERGY OF TWO TUBES FILLED WITH CEMENT MADE AT TWO DIFFERENT WETTING DIE TEMPERATURES 59
FIGURE 4-16 THE ABSORBED ENERGY OF TWO TUBES FILLED WITH CEMENT USING TWO DIFFERENT EXIT PRESSURES 60
FIGURE 4-17 THE ABSORBED ENERGY OF TWO TUBES FILLED WITH CEMENT MADE 61
WITH PRE-OPEN DEVICE AND WITHOUT PRE-OPEN DEVICE 61
FIGURE 4-18 THE ABSORBED ENERGY OF THE TUBES FILLED WITH CEMENT MIXTURE MADE UNDER DIFFERENT WETTING DIE ROTATING SPEEDS 63
FIGURE 4-19 THE VOID CONTENT OF TUBES MADE UNDER DIFFERENT WETTING DIE ROTATING SPEEDS 63
FIGURE 20 THE LOAD VS DISPLACEMENT CURVE OF THE TUBE FILLED WITH CEMENT MIXTURE AND WITH 15 INTERNAL TAPES 65
FIGURE 4-21 THE LOAD VS DISPLACEMENT CURVES OF THE TUBES WITH SMOOTH INNER SURFACE FILLED WITH CEMENT MIXTURE AND REINFORCED WITH 15 INTERNAL TAPES (SAMPLES FAILED AFTER 12 TIMES OF BENDING) 67
FIGURE 4-22 THE LOAD VS. DISPLACEMENT CURVES OF THE TUBES WITH FUZZY INNER SURFACE FILLED WITH CEMENT MIXTURE AND REINFORCED WITH 15 INTERNAL TAPES (SAMPLES FAILED AFTER 23 TIMES OF BENDING)..... 67
TABLE 5-1 THE COMPARISON AMONG TENSILE PROPERTY OF DIFFERENT MATERIALS 69

Chapter I

Introduction

The performance characteristics of reinforced concrete have led to disappointment in some applications. For example, the deterioration of reinforced concrete structures has become a serous problem in the last decade. Reinforced concrete structure such as bridge decks, pavements, parking garages, wastewater treatment plants, port and marine structure are weakening prematurely due to the corrosion of steel reinforcement. The cause of the corrosion is from the significant fluctuation of the temperature, use of salt for deicing, or industrial chemical In Canada, it is estimated that repair cost of parking garages is in the range of $ 6 billion [1]. The estimate of repair cost for existing highway bridges in the U.S. is over $50 billion and one to three trillion for all concrete structures [2]. Excessive corrosion problems also exist in the Arabian Gulf country [3].

The traditional way to fight steel corrosion in concrete is cathodic protection systems and using galvanized or epoxy-coated reinforcing bar [4]. Long term efficiency of these systems is still in doubt [5].

The use of corrosion resistant fiber-reinforced polymer (FRP) rebar offers an alternative to mild steel reinforcement by improving the longevity and durability of structural facilities exposed to aggressive environments. FRP rebars possess several unique advantages for solving engineering problems where conventional materials do not

perform well. Their excellent fatigue behavior, high strength-to weight ratio, high tensile strength, nonconductivity, and thermal expansion closer to that of concrete are among the well-known advantages [6]. A hollow FRP rebar presents even more advantages, such as increased strength-to weight ratio, and provides a system that could be used both as structural elements and conduits [7].

Almost all the fiber reinforced plastic adapted to reinforcing concrete uses thermsetting resins, that have low toughness, need a curing process, and have high fabrication costs. This paper presents a brand new way for producing glass fiber reinforced thermoplastic tubes which can be used to reinforce concrete with high toughness, low cost and time efficiency. The research describes the processing of the hollow tube, optimizing the processing factors, and evaluating the mechanical properties of the hollow tube filled with cement mixture. The information gathered in this investigation is valuable for the future development of the design of glass fiber reinforced thermoplastic tubes used for reinforcing concrete

Chapter II

Literature Review

Portland cement and steel concrete

Portland cement, by definition, is a cementive material which is obtained by intimately mixing together calcareous or other lime-bearing materials with, if required, argillaceous and/or other silica, alumina, or iron oxide-bearing materials, burning them at a clinkering temperature and grinding the resulting clinker.

A few percent of gypsun is added during grinding to regulate the setting time of the cement According, Portland cement consists mainly of lime (CaO), silica (SiO_2), Alumina (Al_2O_3), and iron oxide (Fe_2O_3). The combined content of the four oxides is approximately 90% of the cement weight and they are generally referred to as the 'major oxides'. The remaining 10% consists of magnesia (MgO), alkali oxides (Na_2O and K_2O), titania (TiO_2), phoshorus pentoxide (P_2O_5), and gypsum These are referred to as 'minor constituents' [55]

Concrete is made of basic ingredients of hydraulic cement that is usually Portland cement, mineral aggregate, and water. It also contains some air and some times admixtures or other materials. It is more or less plastic after mixing but subsequently hardens into a stonelike material The aggregate particles in concrete are held together by a hardened cement paste. The strength of ordinary concrete depends to a large extent on

the strength of aggregate to paste bond as affected by water/cement ratio, surface roughness of aggregate and chemical composition of the concrete system. The average strength can be found in Table 2-1.

Concrete is an inherently brittle material, strong in compression but weak in tension and lacking ductility. Steel bars, on the other hand, are strong in tension and quite ductile. Steel reinforced concrete is a combination of both steel and concrete, using the best properties of each. The average mechanical properties of several steels can be found in Table 2-2

Corrosion of steel in concrete

Corrosion of reinforcing steel is a worldwide problem. The mechanism of the corrosion is quite complex because the nature of the portland cement matrix is quite complex. Concrete contains microscopic pores with high concentrations of soluble calcium, sodium and potassium oxides. The alkaline condition leads to a 'passive' layer forming on the steel surface. A passive layer is a dense, impenetrable film which if fully established and maintained, prevents future corrosion of the steel Once the passive layer breaks down then areas of rust will start appearing on the steel surface. Unhydrated ferric oxide Fe_2O_3 has a volume of about twice that of the steel it replaces when fully dense. When it becomes hydrated it swells even more and becomes porous. This means that the volume increase at the steel/concrete interface is two to ten times. This leads to the cracking and

Table 2-1. Average physical properties of building stone, brick and concrete [55]

Material	Density, lb/ft^3 (kg/m^3)	Temp Coef Of Linear Expansion per °F (Temp Coef Of Linear Expansion per °C)	Ultimate Compressive strength, psi (MPa)	Ultimate Shearing strength Across Grain, psi (MPa)	Modulus of rupture in bending, psi (Mpa)	Modulus of Elasticity in compression, psi (Gpa)
Granite	165 (2640)	$3\ 6 \times 10^{-6}$ ($6\ 48 \times 10^{-6}$)	20,000 (137 88)	2,300 (15 86)	1,600 (11 03)	7.5×10^6 (51 7)
Limestone	160 (2560)	$3\ 0 \times 10^{-6}$ ($5\ 4 \times 10^{-6}$)	10,000 (68 94)	1,400 (9.65)	1,200 (8 27)	$8\ 4 \times 10^6$ (57.9)
Marble	170 (2720)	$4\ 0 \times 10^{-6}$ ($7\ 3 \times 10^{-6}$)	12,000 (82 73)	1,300 (8 96)	1,500 (10 34)	$8\ 2 \times 10^6$ (56 53)
Sandstone	135 (2160)	$5\ 2 \times 10^{-6}$ ($9\ 36 \times 10^{-6}$)	10,000 (68 94)	1,700 (11 72)	1,500 (10 34)	$3\ 3 \times 10^6$ (22 75)
Slate	175 (2800)		15,000 1(03 41)		8,000 (55 15)	14.0×10^6 (96 52)
Common brick	125 (2000)	$4\ 0 \times 10^{-6}$ ($7\ 3 \times 10^{-6}$)	4,000 (27 58)		800 (5 52)	$2\ 0 \times 10^6$ (13 78)
Stone or gravel concrete*						
7 5 gals water per sack of cement	150 (2400)	6.0×10^{-6} ($10\ 8 \times 10^{-6}$)	3,700 (25 51)	1,000** (6 89)	550 (3.79)	$3\ 1 \times 10^6$ (21 37)
6 75 gals water per sack of cement	150 (2400)	$6\ 0 \times 10^{-6}$ ($10\ 8 \times 10^{-6}$)	4,300 (29 64)	1,250 (8 62)	600 (4.13)	$3\ 3 \times 10^6$ (22 75)
6 gals water per sack of cement	150 (2400)	$6\ 0 \times 10^{-6}$ (10.8×10^{-6})	5,200 (35 85)	1,500 (10 34)	700 (4 83)	3.5×10^6 24 13)

*Strength values are for concrete 28 days old Working strengths may be taken as one-quarter of these 28-day strengths

**This direct shearing strength must not be used in a beam involving diagonal tension where the concrete may break with a shearing stress equal to from 5 to 10 per cent of its compressive strength

Table 2-2 Mechanical properties of steel (typical value)[56]

Materials	Modulus of elasticity $E\times 10^{-6}$ psi(Gpa)	Shear modulus of elasticity $G\times10^{-6}$ psi(Gpa)	Ultimate tensile strength psi(MPa)	Yield strength (o.oo2 offset) psi (MPa)	Ultimate shear stress Psi (MPa)	Density Lb/in.^{3} (g/cm^3)	Coefficient of expansion $\alpha\times10^6$ strain/°F ($\alpha\times10^6$ strain/°C)
SAE 1020*	28 0 (193)	10 0 (68 94)	55,000 (379)	36,000 (248)	35,000 (241)	0 283 (7 83)	6.5(11 7)
SAE 4130 (normalized)	29 0 (200)	11 0 (75 83)	90,000 (620)	70,000 (482)	55,000 (379)	0 283 (7 83)	6 5(11 7)
SAE 4130	29 0 (200)	11 0 (75 83)	125,000 (861)	100,000 (689)	75,000 (517)	0 283 (7 83)	6 5(11 7)
18-8 stainless	28 0 (193)	9 5 (65 49)	120,000 (827)	80,000 (552)		0 284 (7 86)	9 6(17 3)

spalling observed as the usual consequence of corrosion of the steel in concrete and the red/brown brittle, flaky rust in the bar and the rust stains seen at cracks in the concrete [52].

Depending on the moisture and gases available to form an electrolyte, corrosion may take the form of general rusting, or localized, severe attack known as 'pitting'. Thus external or environmental conditions will also influence the type and rate of the corrosion [53].

- General Rusting· Once corrosion starts, it tends to be self-accelerating. In general rusting, the metal is oxidized in a chemical reaction triggered by contaminants, such as chlorides, and the resulting rust typically occupies eight times the volume of the original steel.

- Pitting Corrosion: This is often a result of chloride ions in the concrete being concentrated in small depassivated areas by the ionic current flow, increasing the conductivity of the electrolytete locally, and so accelerating the pitting process at the small anodic point. The corrosion products are usually deposited over the larger remaining cathodic area, and rapid metal loss occurs at the corrosion pit, but rust may not form sufficient thickness to cause cracking.
- Galvanic Corrosion: Each metal and metal alloy occupies a given position in the 'Galvanic series' [54], signifying an anodic or cathodic nature relative to other metals in the environment. Electrolytic action removes material from the anode, and the further apart metals are in the galvanic series, the more aggressive is this reaction. Therefore two dissimilar metals embedded close together in concrete will react in the same way as steel with surface potential differences, if the concrete is suitably conductive.

Carbonation is one main kind of chemical attack on concrete. As an example of an atmospheric or environmental attack, the carbonation process also shows the interaction that occurs during the deterioration of concrete Cement paste has a submicroscopic pore matrix, and absorbs moisture by capillary action. It ' breathes' with changes in humidity, atmospheric pressure, and temperature. Carbon dioxide penetrates the concrete, to react with the pore moisture, forming carbonic acid. This in turn reacts with the alkaline calcium hydroxide in the cement to form calcium carbonate, reducing the pH of the matrix to around 9.4. By reducing the alkalinity of the concrete in this way, carbonation

can destroy the concrete's ability to maintain the protective oxide layer on any embedded steel, and so open the way for corrosion.

Chloride attack is a another major kind of chemical attack on steel. Free chlorides increase the electrical conductivity of moisture present in the carbonated concrete, and by chemical reaction promotes depassivation of the steel. In doing so, they create both conditions for which the engineer is concerned about conductive concrete and good electrical contact between concrete and steel The chlorides thus take an active part in both destroying the protective properties of the concrete, and in the corrosion process itself [53].

Chlorides can come from several sources [52]. They can be cast into the concrete or they can diffuse in from outside. Chloride cast into concrete can be due to:

- Deliberate addition of chloride set accelerators
- Use of sea water in the mix
- Contaminated aggregates.

Chlorides can diffuse into concrete as a result of

- Sea salt spray and direct sea water wetting
- Deicing salting
- Use of chemical (structures used for salt storage, brine tanks, aquarium, etc)

Fiber reinforced plastics for reinforcing concrete

Fiber reinforced plastics have the characteristics of high strength, light weight, nonconducting, noncorrosive and nonmagnetic. They have been used in lieu of steel for reinforcing and prestressing tendons in concrete beams, columns, bridge deck slabs etc. The FRP reinforcement may be made in rods, bars, strands, two-dimensional grids, three-dimensional grids, gratings, plates, hollow tubes, and wrapping materials (figure 2-1, and figure 2-2). The surface of the FRP can be modified to increase the bond with the surrounding concrete. The methods of production include pultrusion, braiding, and filament winding

The most used fibers in FRP are aramid, carbon, and glass. The aramid and carbon fibers are high modulus, and glass fiber is the cheapest. The glass fiber generally used is either S-glass or E-glass. The resin used as matrix in the FRP is usually a thermosetting resin like polyesters, vinyl esters or epoxies.

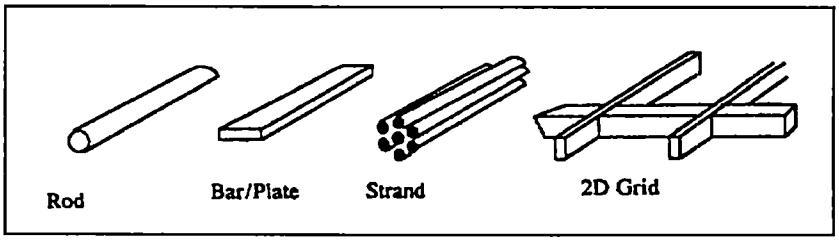

Figure 2-1 FRP reinforcement types

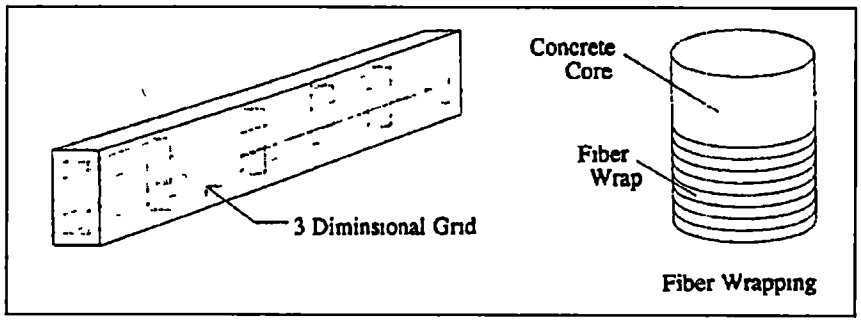

Figure 2-2 Three-dimensional FRP Grid and fiber wrapping

The FRP Reinforcing Bars

Fiber Reinforced Plastic bars are unaffected by electrochemical corrosion and are magnetically inert Therefore, this type of reinforcing bar exhibits good potential for use in structures where corrosion is a problem or places where magnetic field should be considered [14,15,16,17].

Fiber reinforced plastic bars are manufactured by pultrusion as shown in Figure 2-3. In this process, strands of slightly twisted fiber are drawn through a catalyzed vinyl ester resin bath. They are then carefully aligned and pulled through a heated forming and curing die which strips away excess resin to produce the desired rod diameter, with final composition approximately 30 percent volume fraction thermosetting resin and 70 percent volume fraction fiber. A band of fiber is wound around the rod in a spiral, creating the final indented surface that provides much of the reinforcing bars bond strength to concrete [18].

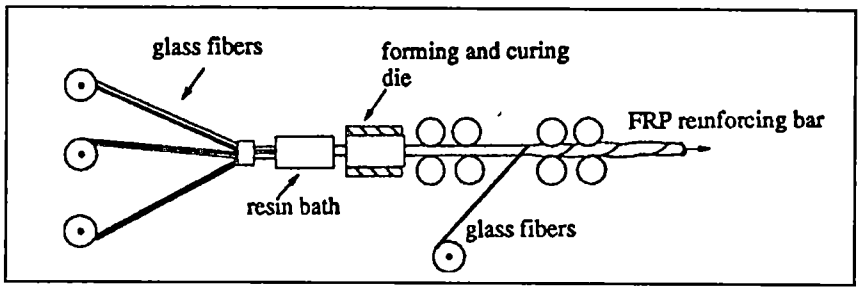

Figure 2-3. Fabrication of FRP reinforcing bar

The matrix material contributes very little to the strength and stiffness of the composite but mainly provides chemical protection and mechanical coupling for the fibers. The mechanical properties of the composite bars depend primarily on the type of the fiber and volume fraction of fiber [19]

The tensile strength of the FRP bar is on the order of 690 to 1100 MPa (100 to 160 ksi) which is higher than that of Grade 60 steel reinforcing bars; while the tensile modulus of elasticity ranges from 40 to 70 GPa(6 to 10 msi), which is significantly lower than that of steel. Shear strength is only about 58.5 MPa(8 ksi)[18]. Benmokrane and Tighiuart[22] reported that the GFRP reinforcing bars ,with fiber content range from 73 to 78 percent by volume and bar diameter range from 9 5 to 25 4 mm (3/8 to 1 inch) have linear elastic behavior up to failure. The average strain at failure is 1.8 percent. The average coefficient of longitudinal expansion is equal to $9\times10^{-6}/°C$. This value is similar to that of hardened concrete and steel reinforcement. The mean tensile strength and modulus of reinforcing

rebars of 12.7, 15 9 and 19 1 mm (½, ¾ and 1 inch)diameter are 683 MPa (99ksi) and 42 GPa (6msi) Malvar[23] did the tensile test on 19 mm(3/4 inch) GFRP bar and found that the strength varied from 448 to 710 MPa(65 to 103 ksi) and the moduli of elasticity ranged from 28 to 48 GPa(4.1 to 6.9 msi).

Bonding of FRP bars in concrete includes three contributing mechanisms: adhesion between the surface of the bar and the cement paste, friction caused by the microtexture on the surface of the bar, and mechanical interlocking producing by the bar deformation In the FRP bars the deformations are smaller, the bond was provided by the friction and adhesion between bar's surface and the concrete. The mechanical interlocking between the bar deformations and the surrounding concrete contribute very little to the bond between the rebar and surrounding concrete [19].

The test methods for the bond of FRP reinforcement included direct pull out, cantilever beam, and notched beam Based on the crack pattern and the predictability of the load-deflection reponses of concrete beams reinforced with FRP bars, Saadatmanesh and Ehsani[20] and Larralde[21] concluded that adequate bonding can be obtained in FRP bars (and ultimate bond stress and load end slip in pull out specimens were significantly greater that the values observed in the beam test). Benmokrane and Tighiuart[22] reported that the bond strength of glass fiber reinforced plastic reinforcing bars varies from 6.4 to 10.6 MPa (928 to 1537 psi) at 0.1 and 0.2 mm (0.004 to 0.008 inch) slip. Those values are lower than that of steel reinforcing bars, approximately 60 to 90 percent of that of steel reinforcing bars, depending on reinforcing bar diameter Malvar[23] found

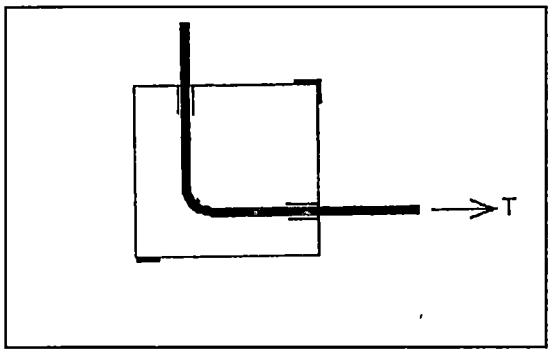

Figure 2-4 The sketch of hooked glass fiber reinforced plastic

that small surface deformations, about 5.4 percent of the nominal rebar diameter are sufficient to yield maximum bond stresses up to five times the concrete tensile strength, similar to that obtained with steel reinforcing rebar, and both surface deformation and indentations obtained by stressing an external helicodial strand are acceptable for bond purposes. Bonding of hooked glass fiber reinforced plastic reinforcing bars (shown in Figure 2-4) to concrete was investigated by Ehsani and Saadatmanesh[24]. They found that more tail length than 12 times the bar diameter had no beneficial effect on the tensile stress, slip, and initial stiffness of the bar, and increasing the straight embedment length of the bars can increase tensile stress and initial stiffness and reduces the slip.Braimah and Green[25] studied polypropylene FRC Bridge deck slabs transversely prestressed with CFRP (Carbon Fiber Reinforced Plastic) tendons. They found that CFRP tendons and polypropylene-fiber reinforced concrete is a feasible alternative to steel reinforced and prestressed deck slabs. And deck slabs transversely prestressed with CFRP rods

proved superior to those prestressed with steel. Michaluk and Rizkalla[26] reported that behavior of the FRP (Fiber Reinfoced Plastic) reinforced slabs through the testing was bilinearly elastic until failure, stiffness of the slabs reinforced by GFRP is significantly reduced after initiation of cracks in comparison to slabs reinforced by steel and CFRP bars

Sanjeev and Kumar[27] investigated fatigue response of concrete decks reinforced with FRP rebars The deck-stringer samples were subjected to cyclic concentrated load at the center of the deck with a load range of 169 1 kN (38000 lbf) and a frequency of 1 Hz. After a maximum of 2,500,000 cycles was applied on the deck, a static test going up to 400.5 kN (90,000 lbf) was applied in an attempt to induce failure in the deck. A 25% to 34% increase in deflection was observed in decks in the fatigue range 0.6-2 million with a maximum central deflection of 0.06 inch(1.5 mm) over 12 ft(3.6 m) span. They found that the gradual stiffness degradation due to fatigue loads in concrete decks prevailed until 80% of their total fatigue life and the deck degradation rate in FRP reinforced decks was similar with steel reinforced decks in the fatigue crack propagation zone. The axial tension fatigue test on the GRFP bars embedded in concrete carried by Adimi and Benmokrane[28] showed the glass-polyester GFRP bar with 73% fibers by weight tested under a stress ratio of 0 1 at a cycling rate of 4 Hz is observed to have a linearly increasing fatigue life as the maximum stress decreased. And it appears from the test that for a desired fatigue life of 4 million cycles, the maximum stress in the GFRP should not exceed 150 MPa(21 ksi), about 22% of its tensile strength

Fiber Reinforced Plastic Grid

Rather than duplicate an existing steel product, some manufactures have taken a different approach to providing FRP reinforcement for concrete structures. FRP grids provide both longitudinal and transverse reinforcement in one unit. For applications such as curtain walls, the use of grids rather than individual bars may result in fabrication and installation efficiencies. In addition, FRP grids resolve problems of poor bond performance of FRP round bars by developing bond through direct concrete bearing members which are placed transverse to the longitudinal axis of the main reinforcing members.[29]

Usually the longitudinal and transverse bars in FRP Grids were fabricated using a process in which bundles of carbon or glass fiber filament were impregnated with vinyl ester resin and then woven in a two dimensional pattern The finished grids were then pressed between heated steel plates which flattened the upper and lower surfaces of the bars [30]. The result of this "built-up" fabrication process is that while the fiber content of the bars is accurately controlled, the bars have an irregular cross section. The fabrication process maintains strict control over the area of fibers, but not over the resin.

Schmeckpeper and Nielsen [31] reported that based on the nominal cross section the failure stress of the FRP grids was 630 to 1280 MPa (91 to 185 ksi) which was significantly higher than the yield stress of steel which is 420 MPa(61 ksi). The modulus of elasticity of the FRP grids was 40,000 to 85,300MPa(5.8 to 12.4 msi), those value were considerably less than 200,000Mpa (30 msi) of the steel. Babthia, and Yan's[32] investigation show some question about usage of FRP grids for reinforced concrete

plates. Under impact, a concrete plate reinforced with FRP grids absorb only 42.31 J(31 ft lbf); this is about a third of the energy absorbed by those reinforced with traditional steel grid. They presume it was due to the brittle nature of the FRP composites. They also found that the use of the high strength concrete can not improve the load carrying capacity of the plate, but can improve the energy absorption capability.

Fiber Reinforced Plastic Plate

Fiber Reinforced Plastic Plates have mainly been used to repair deteriorated reinforced concrete structures as the structure ceases to provide satisfactory strength and serviceability

Fiber Reinforced Plastic Plates were usually made of several layers of woven roving glass fiber embedded in a plastic matrix Woven roving is a coarse glass fabric made by weaving untwisted roving almost in plain weave. The plastic matrix consists of a liquid polyester resin, catalyst and accelerator to set into rigid form [33].

Saadatmanesh[34] reported that fiber glass reinforced plastic plate bonding can be used to increase the flexural strength and stiffness of reinforced concrete beams and that the behavior, strengthened in this way, is very similar to behavior of beam strengthened with steel plate-bonding Sharif and Al-Sulaimna[35] carried out a test which showed repaired beams developing their flexural capacities to 57 to 80 kN(12.815 to 18.000 lbf) as the plate thickness change from 1mm to 3mm, those values can provide enough ductility despite the brittleness of FRB plates. The test result indicated effectiveness of FRP plates

for use as a means of external fortification for damaged or underdesigned reinforced concrete beams.

Hollow fiber reinforced plastic composite column

The hollow fiber reinforced plastic composite column [36] show in Figure 2-5 consists of two kinds of plys; an inner ply of longitudinal fibers and outer ply of circumferential fibers. The longitudinal fibers were held by the outer circumferentially oriented fiber ply and from inward buckling by the concrete core.

The FRP shell can be used as a pour form for concrete, this will save time and the cost of formwork [37]. It can protect concrete and the embedded reinforcing steel in corrosive environments [38]. It improves the column's shear strength, provides external

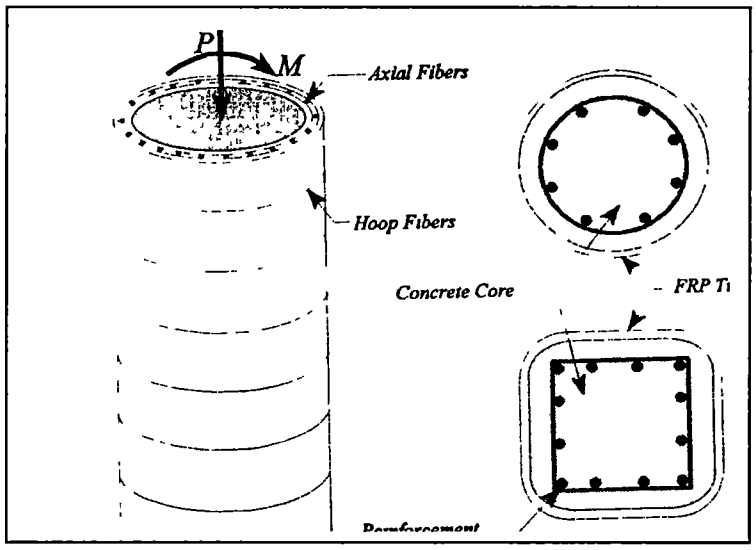

Figure 2-5. FRP-concrete composite column

reinforcement in the circumferential and longitudinal direction, and it increases the flexural capacity of the column similar to concrete-filled steel tubes [39,40,41].

Concrete column reinforced with fiber reinforced plastic strap wrapping

Many bridge failures during earthquakes were caused by inadequate lateral reinforcement and insufficient lap length of the starter bars. Some research [42] reported that closed spaced transverse reinforcement in the potential plastic hinge zone of bridge column increases ultimate compression strength and strain of the concrete core. Priestly and Seible[43] showed that strengthening bridge columns with fiberglass/epoxy jackets significantly improved the flexural and shear strength and increased the ductility of the column In the research carried by Saadatmanesh and Ehsani[44], the concrete columns' diameter is 12 inch(305 mm) and these column were reinforced longitudinally with 14 No.4 bars whose diameter is 0 5 in(12 7mm), resulting in a longitudinal reinforcement ratio of 2.48 percent. The composite straps were made by impregnating glass fiber in polyester resin They were 0.03 inch(0.76mm) thick and had a tensile strength and modulus of elasticity of 532MPa (77 ksi) and 18.6 GPa(2.7 msi). The columns were wrapped with FRP composite straps and tested under reversing inelastic load cycles The result showed that concrete columns externally wrapped with the FRP composite straps in the potential plastic hinge region showed significant improvement in both strength and displacement ductility When the lateral load reached 62 kN(14,000 lbf)), the strain of nonretrofit column in hoop approved 15×10^{-4} However at the same lateral load level, the strain in the retrofit column was only 3×10^{-4}. The retrofit column developed very stable load-displacement hysteresis loops up to a displacement ductility level of u=±6, (u

is the displacement ductility factor defined as the ratio of the applied displacement over the displacement at first yielding of the longitudinal reinforcing bars) without evidence of significant structural deterioration associated with the bond failure of lapped bars or longitudinal reinforcement buckling

Glass fiber reinforced concrete

Glass fiber reinforced concrete is a portland cement-based composite with alkali-resistant chopped glass fibers randomly dispersed throughout the products [45] The glass fiber reinforced concrete was usually applied to the mold by three ways The most common is simultaneously spraying glass fibers and a slurry mix of cement and sand into molds. The glass fibers are about 40 mm (1.57 inch) long. The second method sprays a premixed material that contains glass fiber strands which are about 13 mm (0.5 inch) long The third way is the hand lay-up method, which mixes, forms, and places the materials into a mold by hand [46] GFRC can replicate almost any concrete material but at a much lighter weight. Shah and Ludirdja [45] found that GFRC showed a reduction in flexural strength and toughness when exposed to an accelerated aging environment. Balaguru reported that fiber can contribute to huge crack width reduction and better crack distribution and further more improve toughness under cyclic and impact loading.

Degradation of mechanical properties of glass fiber reinforced concrete over time is a problem [47]. The weakening not only is the result of chemical attack on glass, but also is caused by growth of hydration products at the glass matrix interface[48]. Alkali-resistant magnesium alminosilicate oxynitride glass and alkali resistant porous glass based on

SiO_2-B_2O_3-RO-ZrO_2 were introduced to be used in portland cement concrete[49]. This kind of glass has excellent alkaline durability. This occurs by the formation of a layer on the corroded glass surface. Because of their low solubility in alkaline solution, Mg and Al are the main cationic components of this layer. The layer acts as a diffusion barrier for released ions and lowers the rate of future attack. Some other scientists [50,51] studied using carbon or CaO-BaO-SiO_2-TiO_2 to coat glass fiber, and found it is effective in improving the alkali resistance of the glass substrate.

Thermoplastic composites

Fiber reinforced composites possess four features: fiber, matrix, the organization of fiber in the matrix, and the interface between fiber and matrix [8]. The function of the fiber is to carry load and determines stiffness and strength of composites. The strength properties of composites, except those that are interlaminar dependent, are mainly determined by the fiber strength. Composite stiffness is also dictated by fiber stiffness. The fiber used in thermoplastic composite may be carbon, boron, glass, silicon carbide, alumina, mullite, aramid, or polyethylene.

The property requirements for the matrix material are different than those for reinforcement. The matrix must have relatively low modulus and strength values and comparable or higher ductility. The matrix serves to

1. Keep the reinforcing fiber in correct orientation
2. Protect the fiber from wear and abrasive damage
3. Provide load transfer among fibers. [58]

The composite performance is influenced by the following matrix properties:

- Elastic constants
- Yield and ultimate strength under tension, compression or shear
- Failure strain or ductility
- Fracture toughness
- Resistance to aggressive organic liquids and moisture
- Thermal and oxidative stability

Historically, continuous fiber reinforced plastic systems in application have been dominated by thermoset resin based composites. In the last 7-8 years, great efforts have been placed on combining thermoplastic resin with continuous fiber enforcement to produce thermoplastic composite materials. [58].

Thermoplastics have been under consideration for replacing thermosets as composite matrix materials for quite some time. Table 2-3[59] lists some of the common advantages and disadvantages when compared to thermosets.

One of the primary goals in any manufacturing process is to reduce fabrication costs (i.e., time, labor, and raw materials cost). Thermoplastics have the potential to reduce the time and the amount of labor in their production. Unlike thermosets, there is no need for curing thermoplastics; thus, they have the possibility to reduce the process time. The reduction in labor is due to the ability of thermoplastic processing to become automated, since " hand on " application of a resin is unnecessary [59].

Table 2-3. Thermoplastics versus thermosets

Aspect	Advantage
Viscosity	Thermoset
Temperature	Thermoset
Cycle Time	Thermoplastic
Post cure	Thermoplastic
Repair and Post Forming	Thermoplastic
Storage	Thermoplastic
Toughness	Thermoplastic

Advanced thermoplastic materials have been too expensive in the past to be considered for replacement of thermosets. There is now a bridge between low cost materials and production of high-tech composites. Techniques are now available which produce inexpensive thermoplastic prepregs for cold draping and hot forming that have promising mechanical properties when compared to conventional materials Simple cost analysis has been performed based on the amount of material needed for structural integrity in combination with material price [60]. Although these prepregs are becoming less expensive, there is still a need to reduce material cost for other processing techniques, for example, filament winding.

The advantages of repairing lie with thermoplastics. Since there are weak intermolecular bonds in thermoplastic, they can be easily reformed to correct for flaws. The shelf lives of this reformable plastic are extensively longer than for thermosets. This is true because

they are consolidated insitu [61]. Therefore, thermoplastic products do not require the curing step that is required by thermosets after production.

The fracture toughness (i.e. resistance to crack propagation) of thermoplastics is often much larger than for thermosets [62]. Although thermosets having high degrees of crosslinking provide excellent strength and modulus values, they are often brittle. Thermoplastic resins have no crosslinking, large amounts of free volume, and have high molecular weight These facts allow energy to be dissipated in thermoplastic matrices that would otherwise promote a crack growth in more brittle materials

One main advantage of polymers is the weight saving when compared to other materials. Although acceptable mechanical properties for thermoplastic composites have generally required products with a fiber volume fraction of 0.6 or greater [59], current technologies are being investigated which yield good results with fractions of 0 5 or less [8]. Obtaining these numbers requires a low viscosity [57], therefore, current technology forces one to turn to expensive prepreges that already contain the desired fiber volume percentages to use as start-up materials for processing.

To contemplate thermoplastic as viable ingredient in advanced composite production, consideration must be given to the high temperature applications, as well as the high melt viscosity that will be encountered. There are two areas of concentration in regards to temperature applications for thermoplastics that must be dealt with as insitu process. The temperature must be taken into account to meet the design requirements. The second area of concentration is the usage temperature. Thermoplastic structural uses are generally limited to well below their glass transition temperature [60]. Most thermoplastics retain comparable mechanical properties to thermosets when below their glass transition [59].

Interfaces and interphases in thermoplastic composites

Both short-term and long term properties of a composite depend critically on the microstructure and properties of interface or interphase between the fiber and the matrix. The word "interphase" refers to region where the fiber and matrix phase is chemically and or mechanically combined or otherwise indistinct [64]. The interphase may be a diffusion zone, nucleation zone, chemical reaction zone, a thin layer of fiber coating, or any combination of the above.

The fiber-matrix interfacial adhesion plays an important role in determining the mechanical properties of a polymer composite. A better interfacial bond will impart to the composite better properties such as interlaminar shear strength, delamitation resistance, and fatigue and corrosion resistance. Much work has been done in the characterization of carbon/graphite fiber surface, and a variety of surface coating and modification techniques have been developed to improve interfacial bonding between such fiber and epoxy matrix [65].

Thermoplastics are receiving ever increasing attention as matrix materials in structural composites. Themoplastic composite can be fabricated by novel techniques less cumbersome and potentially faster than thermost curing Thermoplastic composites are also well known for their outstanding impact resistance and damage tolerance However, interfacial adhesion between fiber and thermoplastic is difficult to achieve. The conventional coupling agents such as silanes appear to be much less successful when applied to reinforced thermoplastics. Further the proposed coupling agent theories do not adequately describe the behavior of thermoplastic system [66].

Experimental methods that can be used to characterize the fiber surface include·

- Electron spectroscopy for chemical analysis (ESCA) or X-ray photoelectron spectroscopy (XPS) is employed to determine if any functional groups have been deposited or chemical active sites created.
- Fourier transform infrared analysis (FTIR) can be utilized to determine the chemical modification of fiber surfaces caused by surface treatment.
- Dynamic comtact angles can be calculated from wetting force measurement carried out on an electrobalance
- Scaning tunneling microscopy (STM) and scanning electron Microscope (SEM) can be applied to examine the fiber surface topography (shape, width, and depth of porosity the fiber surface area is important in considering the lock and key configuration between fiber and matrix).
- Thermal desorption method can be conducted to measure the amount and composition of the absorbed species (H_2O, CO, CO_2) that can serve as void generators within the composites.

A necessary condition for the formation of a proper fiber-resin interface is that the liquid resin "wet" or spread on the fiber surface. The contact angle which a drop of liquid forms when placed in contact with a surface is often taken as an indication of the compatibility between these two components. If the contact angle θ formed is less than 90 ° then the liquid is said to wet the solid. At the extreme case where θ is 0°, the liquid is said to spread on the solid substrate. Either wetting or spreading insures an acceptable interfacial free energy for adhesion in that the thermodynamic work of adhesion is positive.

Experimental measurements of contact angles on fibers of approximately 7 μm (0.28 milli-inch) in diameter are difficult to perform optically Contact angle values can be obtained indirectly by immersing the fiber into the liquid and measuring the force of immersion. A simple force balance permits the calculation of the contact angle provided the fiber perimeter and surface free energy of the liquid are known.

If a fiber fractures, the matrix translates the load to the neighboring fibers in the composite, the stress concentration at the broken fiber ends, unless dissipated properly may induce failure on adjacent fibers and precipitate catastrophic failure of the composite Interfacial debonding, caused by the large shear stress at the tip of the fiber end can act to relieve local stress concentrations near a fiber break to avoid brittle failure. On the other hand, the interfacial bond must be sufficiently high to allow effective stress transfer from the resin to the fiber in order to achieve a maximum tensile strength in composites

An early work by Adams and Doner[67] indicated that the application of tension transverse to the fibers induces a maximum tensile stress at the equator of a cylindrical fiber and shear along the fiber axis. Zimmerman and Adams[68] used finite element methods (FEM) to study the transverse failure behavior of composites. They predicted matrix yielding in the region along the 0° direction, which eventual led to matrix cracking and apparent interfacial failure.

The in-situ thermoplastic filament winding process

In filament winding processes, thermoplastic composites open the possibility of combining the laydown, melting and consolidation step in a continuous process [69] In

order to make better production, some have used a laser beam to heat the two mating surfaces of substrate and the incoming tape when the tape ran over a compaction roller and then around a mandrel [70].

The filament winding technique has been examined for continuous-fiber, with thermoplastic prepregs as the start-up materials [59]. The process models for these materials incorporate compaction forces, melt temperature profiles, and take-up winding velocities Material costs and processing speeds (i e 120 ft/min for current composite processing speeds that utilize thermosets as the matrix material) need to be enhanced for these processes to match the present epoxy system [73]. The main problem has been in the time that it takes between the heating of the impregnated tow and consolidation. This limiting factor needs to be overcome by either advancing current heating/consolidation technology or implementing on-line impregnation.

Advances in glass/polypropylene tape laying, which use a robotic arm in the filament winding workcell have been developed to aid faster and more precise production [71]. This research has also yielded composite winding patterns of 90° and $\pm$ 45°(reference direction is cylinder centerline) for composites of a pre-determined length. According to Sayre, a filament winding process still has not been developed which incorporates as uninterrupted product, a raw material start-up, and bias angle winding pattern [72].

In a filament winding process, either fiber tows impregnated with matrix or narrow tapes containing fibers and matrix are wound on a mandrel. Temperature and pressure are applied either continuously as the tows or tapes are being wound or after the winding of the entire structure has been completed. In all of these processes it is important that the proper temperature and pressure should be applied, otherwise composite properties may

suffer· crystallinity may be non-uniform, the plies may not be consolidated and the residual stresses and strain may be unacceptable [62]. In the study of Hummler[71], it is said that three processing parameter-nozzle temperature(the temperature of the filament when it just will be wound on the mandrel), mandrel speed, and consolidation force-have significant influence on the quality of ring wound from glass/polypropylene material. Three main observations were made:

- the shear strength of composite decreases with higher mandrel velocity
- the shear strength of composite increases with higher nozzle temperature
- the influence of the consolidation pressure on the shear strength of composite is minimal

The mandrel temperature also has a great influence on the production quality [76]. The tension on the filament when it is wound onto the mandrel is important. The molten matrix was able to flow around fibers and adequate wetting was achieved. So adding pressure onto the mixer of matrix and fiber may be a useful way to increase wetting [77].

Bias angle wraps play a major role in the strengthening of composite. Composites that are wrapped in a 90° wrap will show great strength in compression and tension in the fiber direction. However, when these composites are tested in applications that do not lie in the reinforcement direction (i.e. transverse tension and bending, they will fail readily. A method must be devised that can increase the failure strength of the product by varying this bias angle wrap[74].

A composite cylinder may have optimized strength in both the longitudinal and hoop directions. Such a cylinder must consist of an optimum bias angle wrap. This bias angle wrap can be determined by developing the following model [63]:

$$f=Pr/t \sin^2\theta, \qquad (1)$$

Where f is the force applied to the cylinder

P is the internal pressure against the cylinder

r is the inner radius of the cylinder

θ is the bias angle wrap from the longitudinal axis

t is the thickness of the cylinder wall

Let f_1 be the hoop stress and f_2 be the longitudinal stress, then:

$$f_1 = f \sin^2\theta \text{ and } f_2 = f\cos^2\theta$$

Now, let the hoop stress be equal to the longitudinal stress and solve for θ. The result shows that the optimum angle for reinforcement in both the hoop and longitudinal direction is 54.7°. By using this model it also shows that when the angle is 90° the composite can withstand greater hoop stress relative to longitudinal stress. When the angle approaches 0°, the composite can withstand greater longitudinal stress.

Varying bias angle (between 0° and 90°) is a way that can add strength and stiffness to a composite in loading that is not in the direction of the reinforcement When angles are varied from ply to ply, shear coupling must not be ignored, or significant deviations from the predicted modulus calculations will occur [74]. The varying of bias angles from ply to ply can also affect predicted values of the strength It has been recorded that as the angle is varied from 0° to $\pm$ 45°(the direction of load is in the 0° direction), the strain at failure is actually several times larger than what is predicted from corresponding unidirectional composites [74]. At greater angles the opposite is known to occur A process must be developed which can produce a product with a bias angle wrap that promotes greater mechanical properties under loading applications.

As a study done in our lab prior to the current work, Sayre [72]did a lot of work about the the effects of angle and fiber volume fraction on the mechanical properties of filament-

wound polyproylene-glass tubes. Fig2-6 shows a general block diagram of his experimental setup.

Computer-aided control was placed on the experimental setup. The computer controlled the action of the tensioner and the translating delivery eye. The speed of the mandrel was controlled by a DC controller that was manually adjusted to the desired RPM. The fiber bundle was fed through the tensioner where the computer-driven stepping motor would activate a brass plunger. This plunger would push the fiber bundle against a piece of rubber tubing while the bundle was being pulled in order to vary the tensioning force and periodicity. Once the fiber bundle went through the die, it was impregnated with

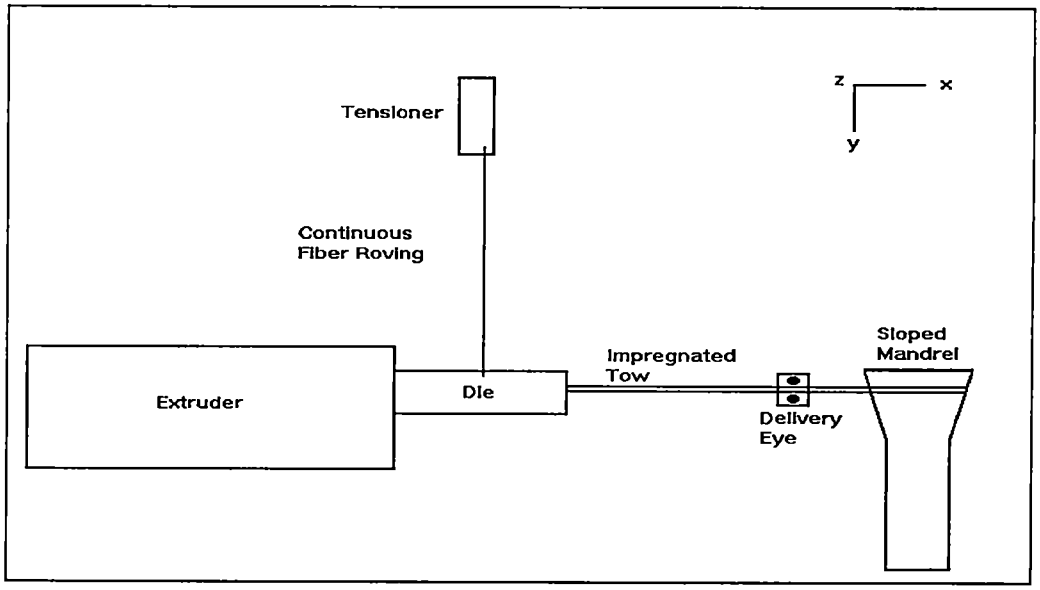

Figure 2-6 General block diagram of Sayre's experimental setup

polypropylene The impregnated tow then proceeded though the delivery eye and onto the mandrel

Tensioning was variably controlled to induce a translational movement in the composite product This motion occurred because the increased tension would reach a value that promoted a slippage of the composite down the sloped portion of the mandrel.

Chapter III

Experimental

Objective

Tubes with 13 inches length and about 2.1 inch diameter were made in order to study the following processing factors (See Figure3-1).

- Mandrel Temperature
- Wetting Die Temperature
- Wetting Die Speed
- Exit Gate Pressure
- Usage of Pre-Open Device

A Three point bending test was used to study the mechanical and fatigue properties of the composite. The tubes were cut vertically, polished, and observed through a microscope The void content and the distribution of the glass fiber were studied through image analysis

Materials

The raw materials used in this experiment were glass fiber, polypropylene, Portland cement and sand. The glass fiber was in the form of roving produced by PPG Industries, Inc Its type is HYBON 4224 and made from E-glass The glass fiber is relatively

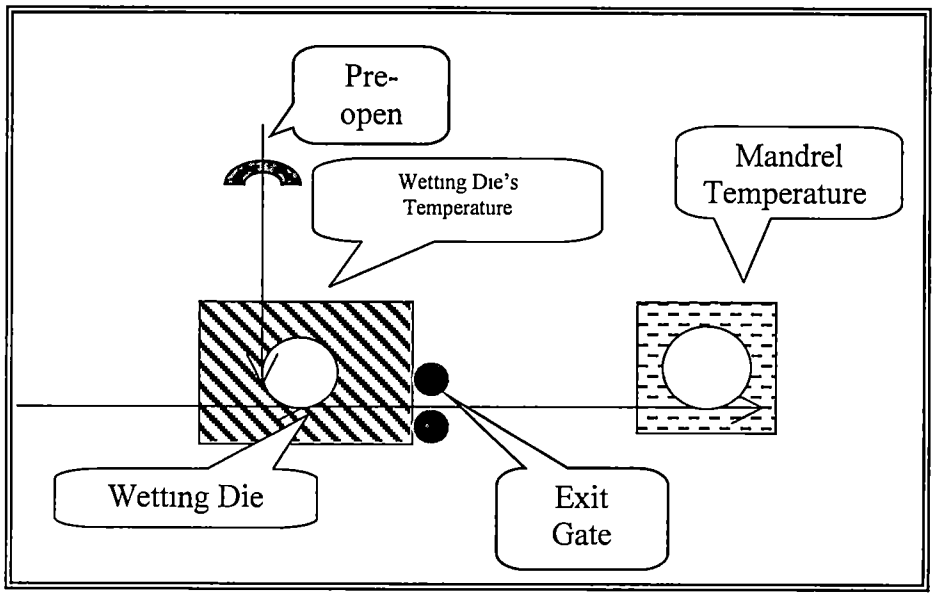

Figure 3-1 Processing factors

inexpensive, isotropic, has high tensile strength and modulus and high chemical resistance, making it a desirable materials for use in composites

The glass fiber used for this thesis had the physical properties shown in Table 3-1 [57].

Table 3-1. The glass fiber's physical properties

Density	2 54 g/cm^3 (0 092 lb/in^3)
Tensile strength	300,000 psi (2068 MPa)
Tensile modulus	12,000,000 psi (82 GPa)

The polypropylene has desirable inherent characteristics, which justifies its use,

- Good chemical, moisture, and heat resistance
- Inexpensive
- Low density
- Good flex life

The polypropylene used for this thesis had the following physical properties shown in Table 3-2 [78].

Table 3-2 Polypropylene's physical properties

MFR	35
Density	0.9 g/cm^3 (0 033 lb/in^3)
Melting Point	160-175 °C (320-347°F)
Glass Transition	-20°C (- 4°F)
Extrusion Range	200-260°C (392-500°F)
Tensile Strength	4,500-6,000 psi (31~41 MPa)
Tensile Modulus	165,000-225,000 psi (1 14~1 55 GPa)

The cement mixture was composed of the Portland cement (HOLNAM, Type 1/1P, Grey), Sand (BONSAL, all purpose) and distilled water

Processing Equipment

- A laboratory scale extruder
- A brass fiber-wetting die
- A plastic based, pre-open device
- A brass mandrel
- An aluminum heating block for the mandrel
- A base made of aluminum that supported the mandrel

- Two motors and controllers
- Three temperature controllers
- Some heating equipment

Figure 3-2 shows a general block diagram of the experimental setup, Figure 3-3 and 3-4 show more details of the wetting and winding facility.

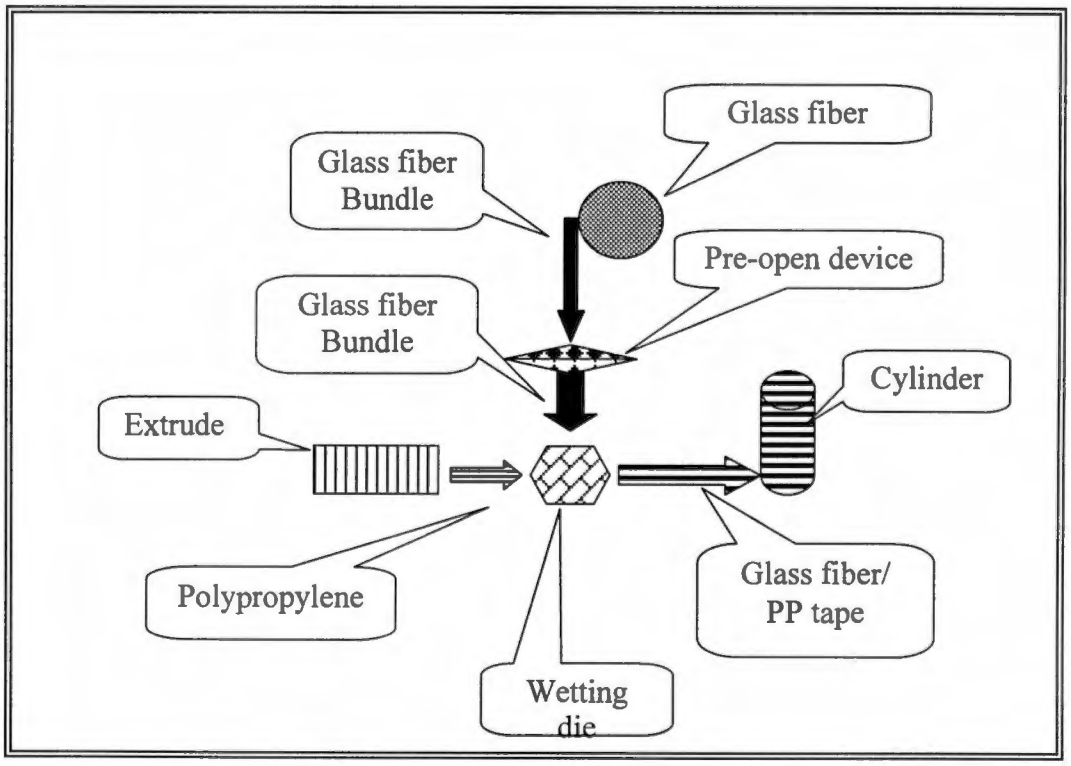

Figure 3-2. General block diagram of experimental setup

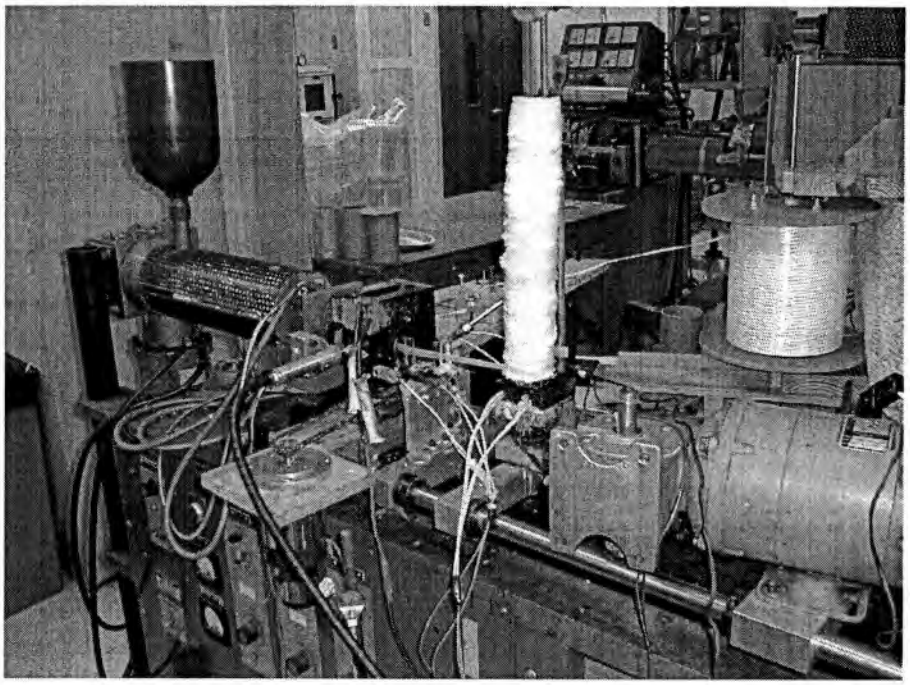

Figure3-3. A photograph of the complete winding facility

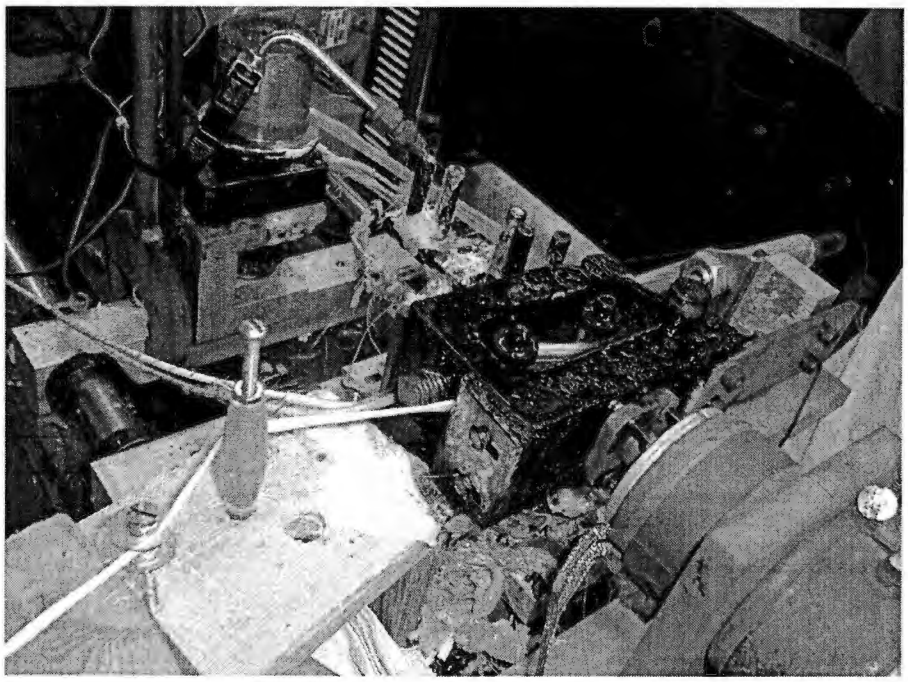

Figure 3-4. A close-up of the pre-open device, wetting die and the mandrel

Routine of Processing and Testing Methods

Processing procedure of the hollow composite column

Figure 3-5 is a simplified view of the components in the process. The process proceeds as follows:

1 Hot, liquid polypropylene at 220°C from an extruder comes into the wetting die through a hole.

2. After being untwisted and spread by the pre-open device, clean fiber glass "yarn" comes into the wetting die through a slot, contacts the polypropylene and passes over the fiber wetter.

3. The fiber-wetter is enclosed in a metal tank, which hold a certain mount of the polypropylene melt.

4. The metal tank is kept at a constant temperature with electric heaters.

5. The completed fiber glass/polypropylene tape exits the wetting die through a pressure controlled exit gate, which adjusts the amount of the polypropylene melt brought out by the tape

6. The mandrel is where the tape is wound on and the composite cylinder is formed. It rotates in the same direction as the fiber-wetter and the electric heater maintains its temperature A DC motor controlled its rotation rate.

7. The glass fiber bundle is pulled the through the wetting die by the mandrel; the impregnated bundle is wound on the mandrel to form the hollow tubes.

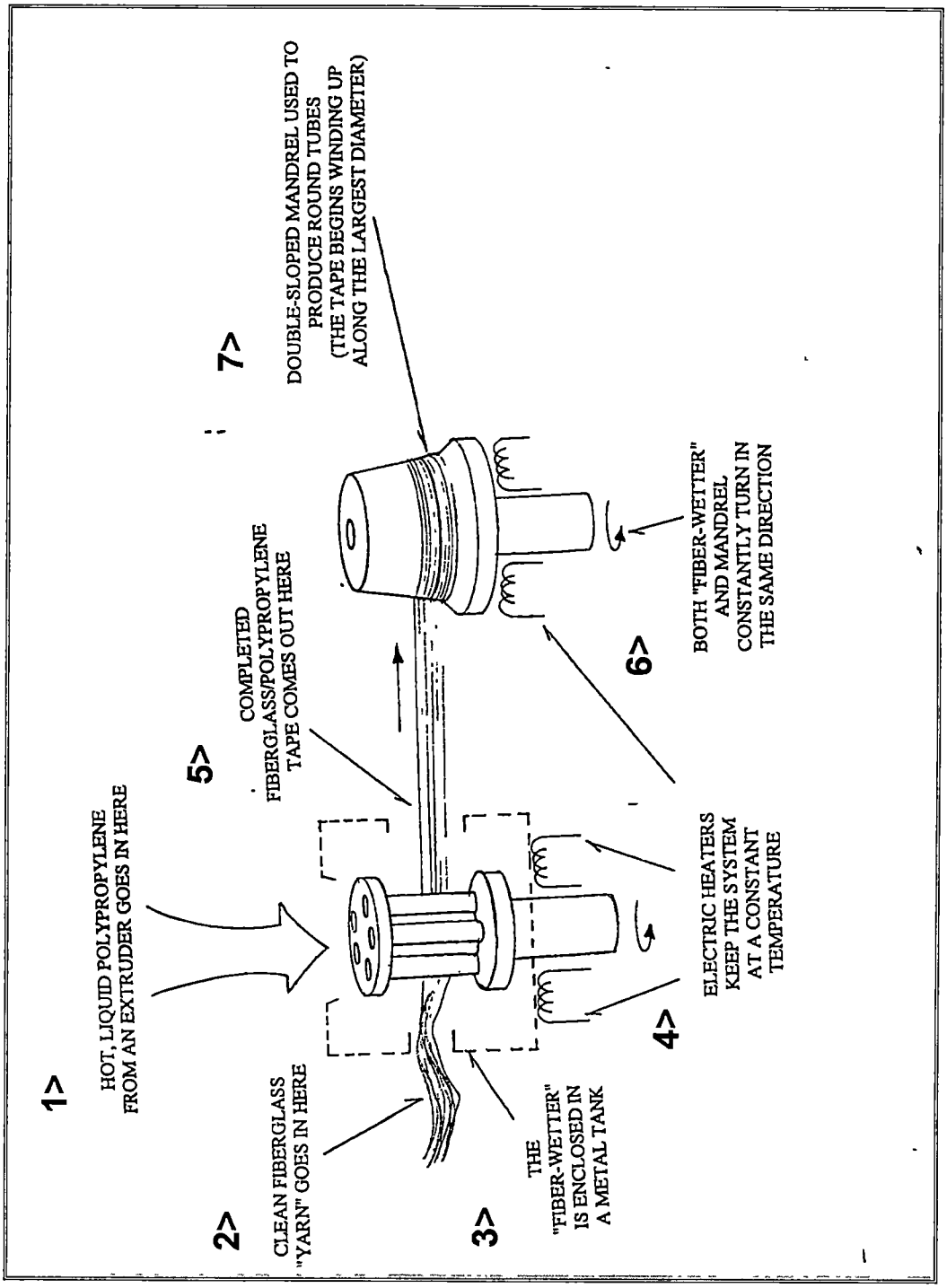

Figure3-5 The diagram processing procedure of the hollow composite tubes

8. The double-sloped mandrel used produces round tubes, its top diameter is a little smaller than the bottom diameter. Under the tension on the tape and the friction force between the tape and the surface of the mandrel, the composite gradually slides off the smaller end, and forms the tube It is possible to make the tubes of any length. As the top diameter of the mandrel is 2 inch(50.8mm), so the hollow tube's inner diameter is about 2 inch (50.8mm) and with a wall thickness of about 0.1 inch(2.54 mm).
9. the composite fiber glass/polypropylene tapes were produced following step 1-5, instead of step 6, the tapes were cooled down by air and cut into 12 inch long section

Reinforcing the cement mixture with tube

The hollow tubes were cut into 10 inch long sections. The cement mixture was made according to formula as Portland cement: sand: water = 2 : 1 : 1 25 parts by volume.

After the cement mixture was prepared, it was be poured into the hollow tubes. The tubes filled with cement mixture were kept in the lab for 30 days before testing. Some samples were prepared by placing 15 15-inch long tapes internally in the tubes to reinforce the structure longitudinally.

Three points bending tests

Three point bending tests were performed on all 10 inch(254mm) long cement filled composite tube samples by using a floor model TTD instron-testing machine. The span

for the two bottom supports is 6 inch(152.4 cm). For more accurate result, 100 pounds (444 8 N) preload were applied to the samples. The bending modulus, first maximum stress, and the absorbed energy of each sample were obtained. Three specimens were tested for each experimental condition studied

Sample polishing and microscopic observation

The hollow tubes were cut into 2 inch (50.8mm) long sections, and then they were cut in half longitudinally. The surfaces vertical to the fiber's direction were polished by 100# sand paper, 600# sand paper, and alumina particles. The surfaces were observed under optical light microscope. The optical light microscope used in this research is Nikon model Epiphot, with lens of 50X, 100X, 200X and 400X. The sample stage of the microscope is above the lens. All the photomicrographs were taken at 50X.

Nonuniformity analysis of glass fiber distribution

Nonuniformity spectra provide a measure of the glass fiber dispersion's uniformity as spatial resolution is varied. Spatial resolution is varied by dividing an image into cells of various sizes ranging from one cell per image to total number of pixels in the image. Glass fiber dispersion uniformity is evaluated for each cell size by computing the coefficient of variation (CV) among the number of the glass fiber in the cells

Examination of Photomicrograph

1 Scan photos of the sample into computer.

2 The analysis software used is "Image Tool"

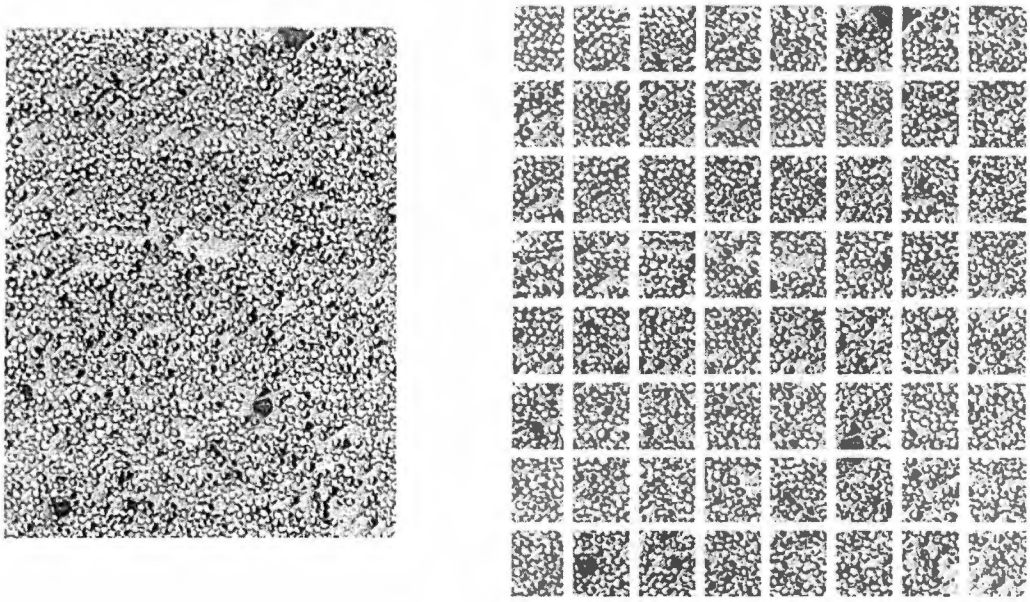

Figure 3-7. An example of how the ¼ photo was split in to 8×8 pieces

3. Use the software "ignite" to split the photo into 16×16 (256) pieces with same width and length. (See Figure 3-7)
4. Use the "Image Tool" to enhance the contrast and the glass fiber's edge in each piece of the split photomicrograph.
5. Use the "Image Tool" to count the number of the objects in every little piece of photomicrograph.

The algorithm for obtaining nonuniformity.

The algorithm for obtaining nonuniformity spectra first divides an image into N divisions along the row and column direction to yield N^2 non-overlapping image cells [75].

The total glass fiber dispersion CV denoted by CVt and was computed using the following Expression:

$$CV_t = \frac{1}{u_m}\sqrt{\frac{1}{N^2}\sum_{i=1}^{N}\sum_{j=1}^{N}(u_{ij} - u_m)^2} \qquad (2)$$

where u_{ij} = the number of glass fiber of cell ij

u_m =mean number of the glass fibers among all cells

N^2=number of cells.

Plots of CVt versus cell size, called glass fiber dispersion nonuniformity spectra were made.

The study for void amount within Sample's cross-section

1. Scan the photos of samples into computer
2. Change the photo from 256-color format into 256 gray-level format.
3. Using the "Threshold Tool" provided by "Image Tool" to select the void areas which appears as red in Figure 3-8
4. Get the amount of the void area from threshold dialogue box showed in figure 3-9

Fatigue test

The fatigue properties of the tubes filled with cement mixture and reinforced with internal tapes were examined by using a cyclical three point bending test. The samples were subjected to a repeat concentrated load at the center of the tubes. The applied load

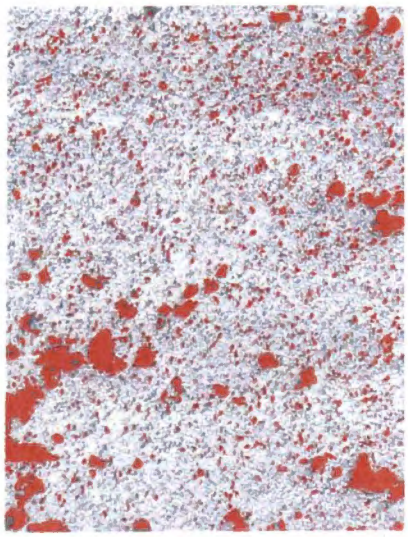

Figure 3-8. The void area selected by the "threshold Tool"

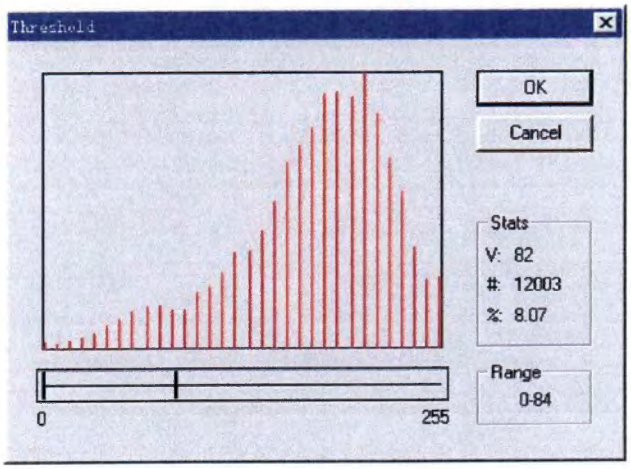

Figure 3-9. Threshold dialogue box which shows the Figure 3-8 has 8.07% voids

was 2,500 lbs(11.12 kN), which is about 50% of the maximum load the samples can withstand. The three point bending test of the samples was repeated until the sample failed. The span of the test is 6 inch, the number of internal tapes was 15.

Chapter IV

Result and Discussion

The results and discussion are presented in six sections They are "The mandrel temperature's effect", "The effect of the wetting die temperature", "The effect of exit gate pressure", "The effect of the usage of the pre-open device", "The effect of the wetting die's rotating speed", "The Reinforcement of internal tapes to the tubes filled with cement mixture" and " Fatigue test". Each topic will be discussed in turn.

The effect of mandrel temperature

The mandrel temperature plays a key role in the processing of the composite cylinders, and along with the mandrel rotating speed determines the tube's consolidation process As show in Table 4-1, the mandrel temperature ranged from 140 to 165 °C. The 140 °C and 165 °C are minimum and maximum temperature at which tubing can be made on the mandrel. When the temperature was below 140 °C, the polypropylene contained within the tape would cool down and adhere on the surface of the mandrel This would stop the tape sliding off and prevent the formation of the tube. When the temperature was higher than165°C, the viscosity of polypropylene within the tape was too low. The composite tapes would just slide off the mandrel and not have enough time to consolidate; there was not enough strength to support the weight of tube which had formed above the mandrel. Overlaps would occur and cause the product to build a "ridge" over time. This "ridge" gave the tube a corrugated appearance which increased as the tube production

continued. Over time the tube no longer appeared to be a constant diameter cylinder, which was the desired product for this study.

Other processing factors shows on Table 4-1 were held constant in order to make it easier to study the effect of the mandrel temperature. Most processing factors were in the mid range in which the machine or material allowed. For the mandrel speed, 10 rpm was chosen; this speed kept the process in a productive speed range and provided enough time for wetting between the polypropylene and glass fiber. It also prevented excessive fiber damage. For the wetting die temperature, wetting die speed, exit gate pressure, usage of pre-open device, they were optimized in another set of experiments.

Inner surface of tubes made using different mandrel temperatures

Through observation of the tubes produced, a huge difference can be easily found between the tubes produced at different mandrel temperatures. As the mandrel temperature increased from 140 to 165 °C in 5°C steps, the inner surface changed from

Table 4-1. Experimental plan for the study of mandrel temperature effect on mechanical properties of the tube filled with cement

No	1	2	3	4	5	6
Mandrel Temperature(°C)	**140**	**145**	**150**	**155**	**160**	**165**
Mandrel speed(RPM)	10					
Wetting die temperature(°C)	180					
Wetting die speed(RPM)	30					
Exit gate pressure(bar)	2					
Usage of pre-open device	Yes					

pretty smooth to fuzzy, then to the condition at which a lot of the glass fiber spread out within the tube, Figure 4-1 presents photographs of four tubes made at different temperatures and the change in the internal surface

When the mandrel temperature (140 °C) is a little lower than the PP's melting temperature, the tape wound on the mandrel can cool down but will not 100% consolidate, so the tape can still slides off the mandrel and keep all the fiber within the polypropylene matrix. After the tape slide off the mandrel, the polypropylene can consolidate and form the smooth inner surface. When the mandrel's temperature increases to 145°C, the polypropylene's viscosity will decrease slightly. Under the tension on the tape, the polypropylene would be squeezed out from between the tapes and the mandrel surface, and a certain amount of void formed among the tapes which had contacted the mandrel surface Then the inner surface become fuzzy, when the mandrel temperature increased further more to 155 or 165 °C, the polypropylene's viscosity will decrease significantly. The polymer matrix cannot hold the glass fiber anymore. After sliding off the mandrel part of glass fibers would spread out into the hollow tube

Mechanical properties

Figure 4-2 shows the load-displacement curves in the three point bending test with four samples made under different mandrel temperature These four samples are filled only with cement mixture

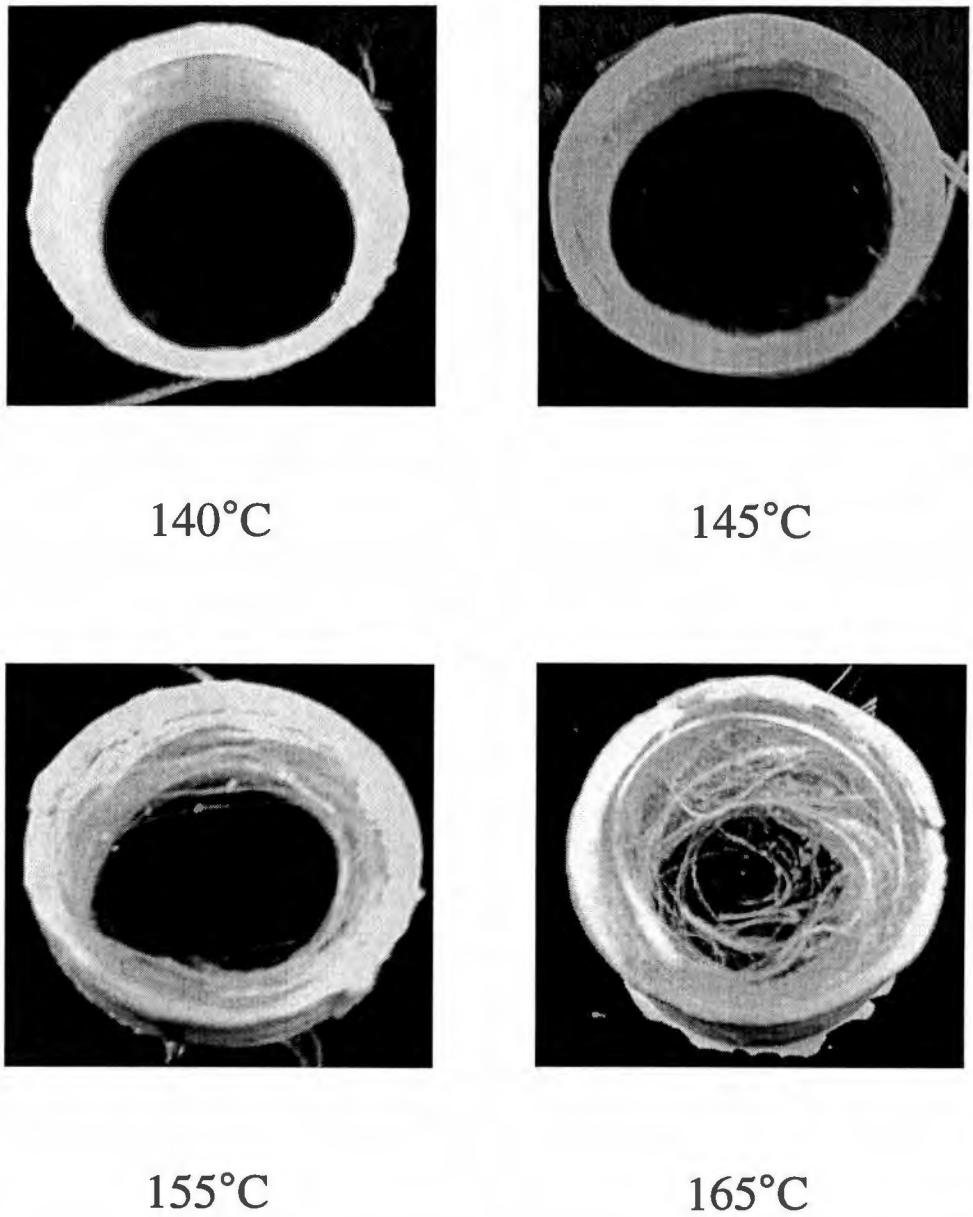

Figure 4-1. Different inner surface appearance of the tubes made under different mandrel temperature

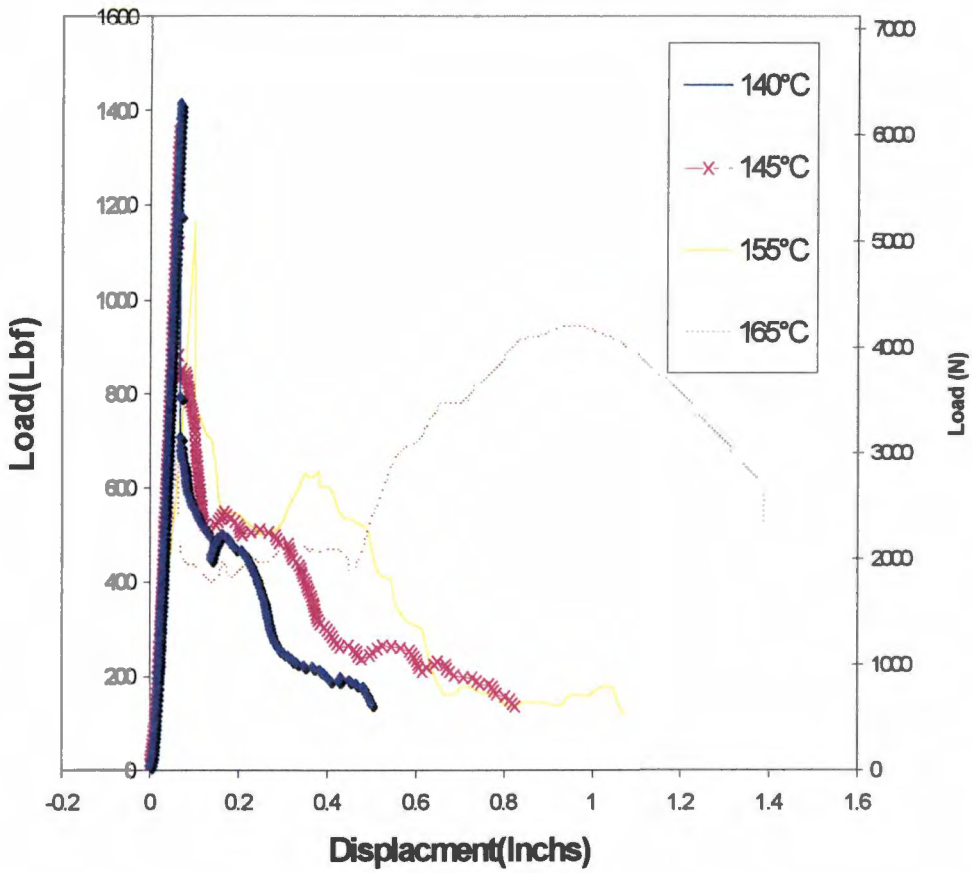

Figure 4-2. The three point bending test for the cement filled cylinder produced with four different mandrel temperatures

Table 4-2 summarizes the change of displacement of tubes made under different mandrel temperatures. In the three point bending test, as the mandrel temperature increased from 140 °C to 165°C the displacement prior to failure increased from 0 499 inch to 1.386 inch(12 7 mm to 35.2mm) over the 6 inch (152.4) span. That number is many times that obtained from conventional structures. It was observed that the cylinder made at a higher mandrel temperature did not fail by sudden catastrophic fracture, but developed progressive damage while maintaining a large amount of load carrying capacity

Explanation for the huge displacement is found by examining the fracture surface of the composite As show in figure 4-1, the tubes made at higher mandrel temperature have a lot of glass fiber spread out in the tube. After the cement mixture was poured into the tube, the cement would impregnate the spread out glass fiber. As figure 4-3 showed, they're about 0.2 to 0 4 inch (5 to 10 mm) thick and appear as a white ring between the shell of the tube and pure cement This ring is formed by the combination of cement and the spread out glass fiber. Figure 4-4 shows the side views of this compound

Table 4-2 The displacements of different tube filled with cement made under different mandrel temperature

Mandrel temperature°C	140	145	155	165
Displacement(inch)	0.499	0.826	1 071	1.386
Strain	0 166	0 275	0 357	0.461

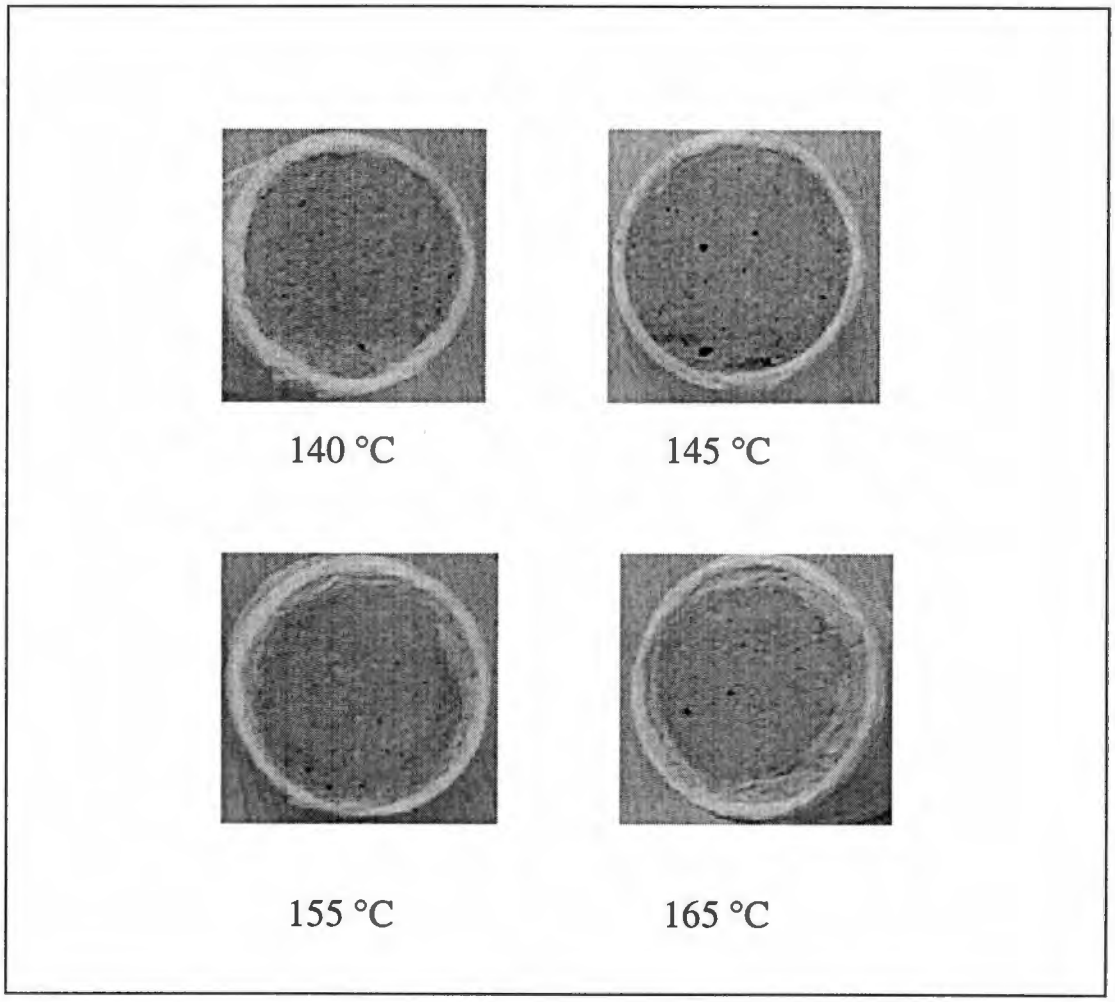

Figure 4-3. The fracture surface of the tube filled with cement made at different mandrel temperatures

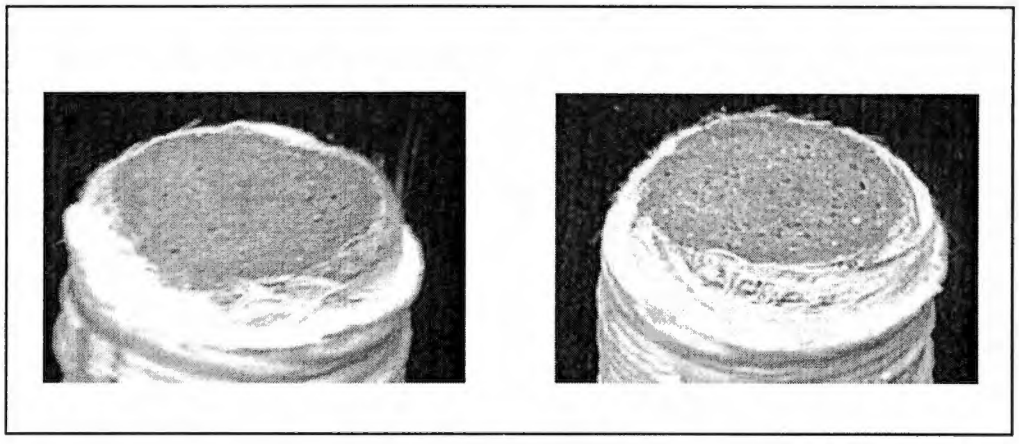

Figure 4-4. The side-view of the fracture surface of the tube made at mandrel temperature 165°C

region after all layer of the tape around the break area were peeled off. It clearly shows that a substantial amount of the glass fiber was embeded in the cement. By this unique structure, the matrix of cement has been bonded to the interior surface of the tube. After the cement core cracks at a small displacement, the cement is still bonded to the tube, through the impregnated fiber, and the load is transferred to the tube shell, and the load would still be carried at high displacement. This benefit results from having continuous glass fiber coated with polypropylene embedded in the cement.

The Elastic modulus

The relationship between the elastic modulus and the mandrel temperature is summarized in Figure 4-5.

The cylinder's modulus was calculated as below:

Stress: $$f = \frac{8Wl}{\pi d^3} \quad (3)$$

Strain: $$\varepsilon = 6\frac{d\delta}{l^2} \quad (4)$$

Modulus: $$E = \frac{Wl^3}{48I\delta} = \frac{4Wl^3}{3\pi d^4\delta} \quad (5)$$

Moment of inertia $$I = \frac{\pi d^4}{64} \quad (6)$$

Where d is diameter of the cylinder

W is the load

L is span distance

δ is displacement

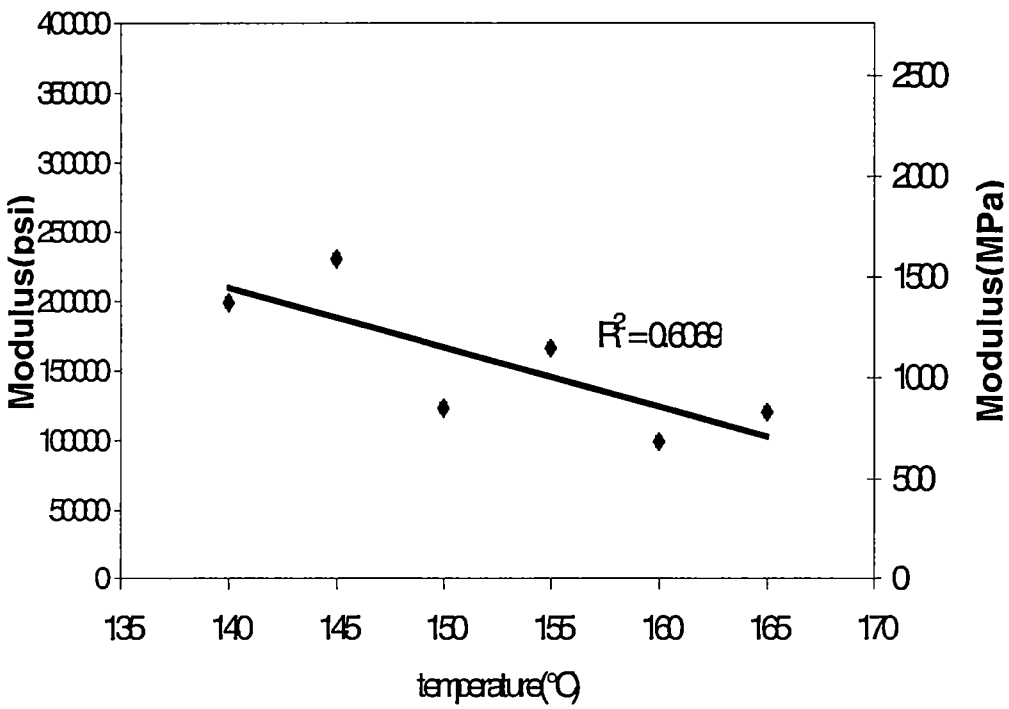

Figure 4-5 Elastic modulus of the tube filled with cement made under different mandrel temperatures

As the mandrel temperature increased from 140 °C to 165°C, more and more glass fiber would spread out within the tube. When the cement mixture was poured in the tube, those glass fiber would produce some void within the cement matrix, the structure of the cement would be damaged, and the elastic modulus of the cement core is lowered.

The Absorbed Energy

The area under the load- displacement curve (figure 4-2) in the three point bending test can be interpreted as the energy absorbed during the test. Figure 4-6 shows the relation between the energy absorbed by the tube and the mandrel temperature.

As the mandrel temperature increased, more and more the glass fiber were embedded in the cement matrix Through the glass fiber's breakage, debonding and slipping, more energy was absorbed by the tube.

The microscopic observation

Under microscopic observation, Figure 4-8 shows that some big pure polypropylene islands existed in the sample at low mandrel temperature. At 140°C, the speed of PP's squeeze flow may be very slow. Extra polypropylene within tapes does not have enough time to flow out from between the tapes, so pure polypropylene island are formed between the layers of glass fibers.

As Figure 4-7 shows, when the mandrel temperature is higher than 145°C, 0 2-0.5(5 – 12.7 mm) inch thickness of pure PP on the outer surface of the cylinder were observed.

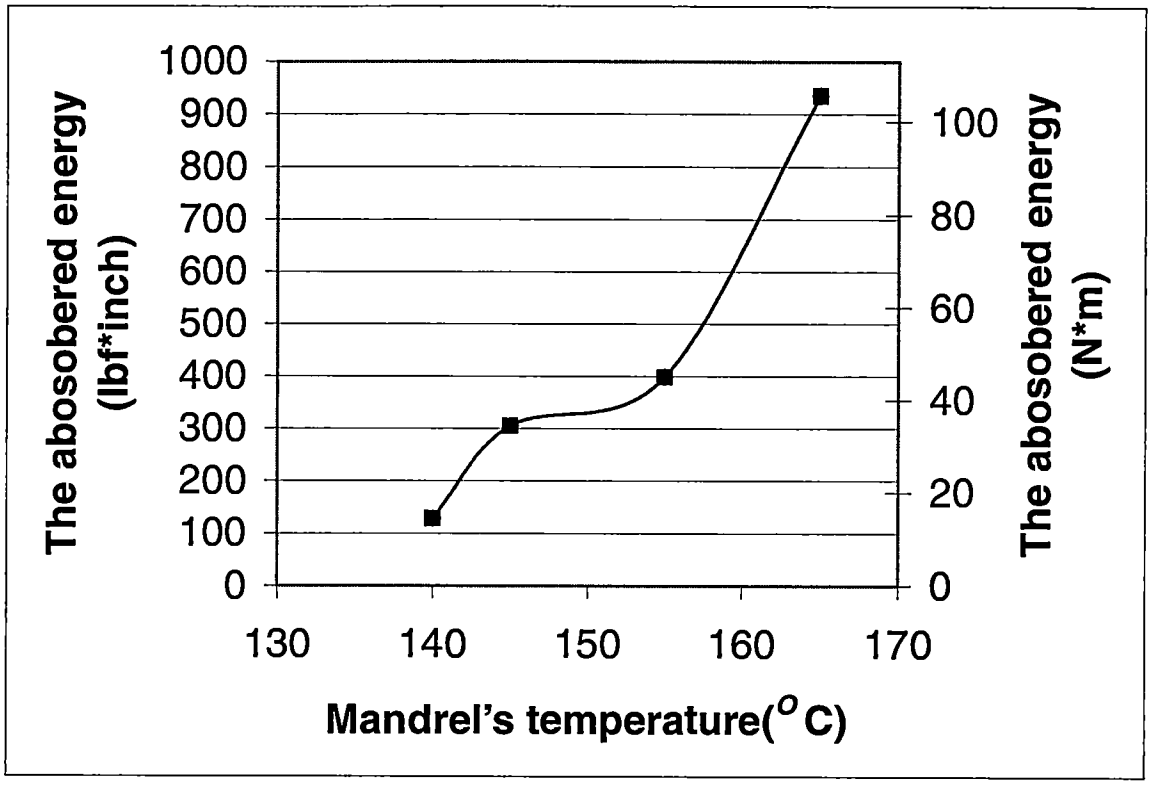

Figure 4-6 The absorbed energy of the cement mixture filled tubes made at different mandrel temperatures.

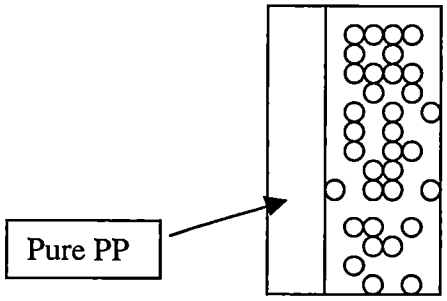

Figure 4-7. Cross-section of the tube processed at high temperature

This phenomenon might be caused by the high quantity of the polypropylene squeeze flow, the PP was squeezed out of the glass fiber layers and gathered outside of the cylinder and deplete the PP islands between the glass fiber layers.

Figure 4-8, 4-9, 4-10 and 4-11 are optical microscopic photos of tube cross-sections processed at various mandrel temperature. The microscopic photos show the glass fiber were distributed within whole island, and these microscopic photos do not show the presence of interlaminar voids, indicating that good intimate contact was achieved between plies. The void content is shown in Figure 4-12. As the mandrel temperature increased from 140°C to 165°C, the void content decreased significantly, from about 15% to less than 5%. Within the composite structure, the void is the place the stress concentrates, less void content can give the structure higher modulus and better mechanical properties

The glass fiber's distribution within the polypropylene matrix.

Figure 4-13 shows the Coefficient of Variation Spectra of glass fiber distribution of tubes made at different mandrel temperatures. The distribution of the glass fiber was distinguishably less uniform for the sample processed at 140°C than for the other three samples which are processed at higher mandrel temperature. But there was not a big difference within the samples made at mandrel temperatures higher than 145°C.

Figure 4-8. Microscopic photo of a cross-section of a 140°C (50×)

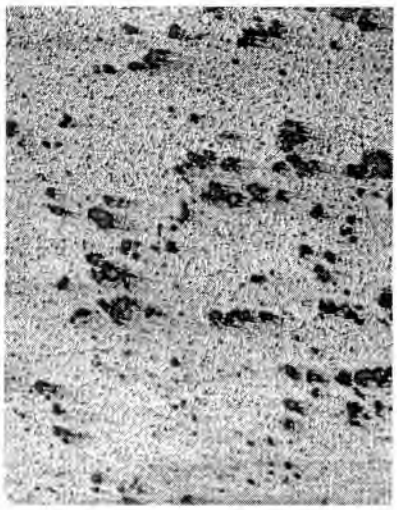

Figure 4-9. Microscopic photo of a cross-section of a 145°C (50×)

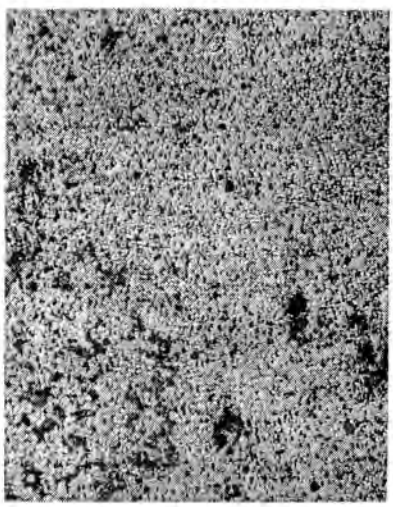

Figure 4-10. Microscopic photo of a cross-section of a 155°C (50×)

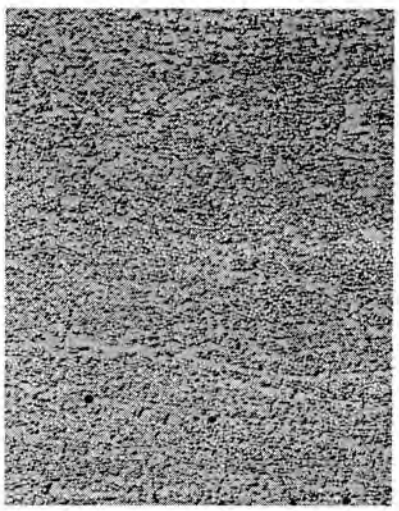

Figure 4-11. Microscopic photo of a cross-section of a 165°C (50×)

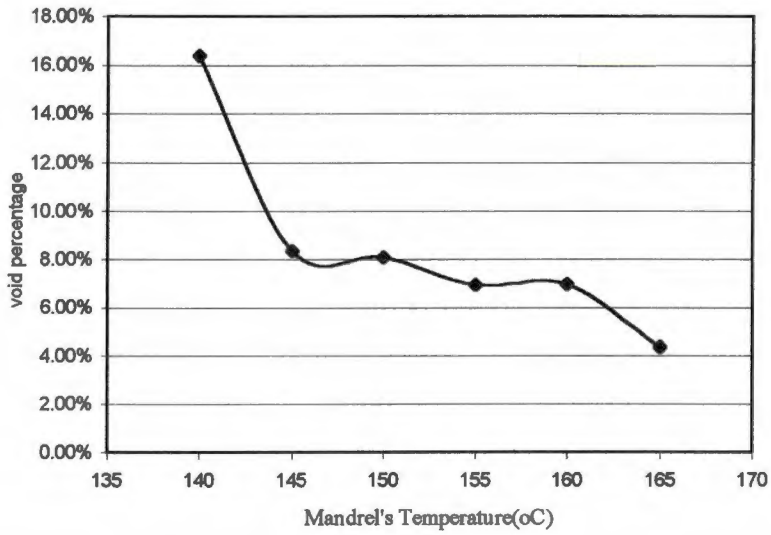

Figure 4-12. The percentage of void in the tubes' cross-section made under different temperatures

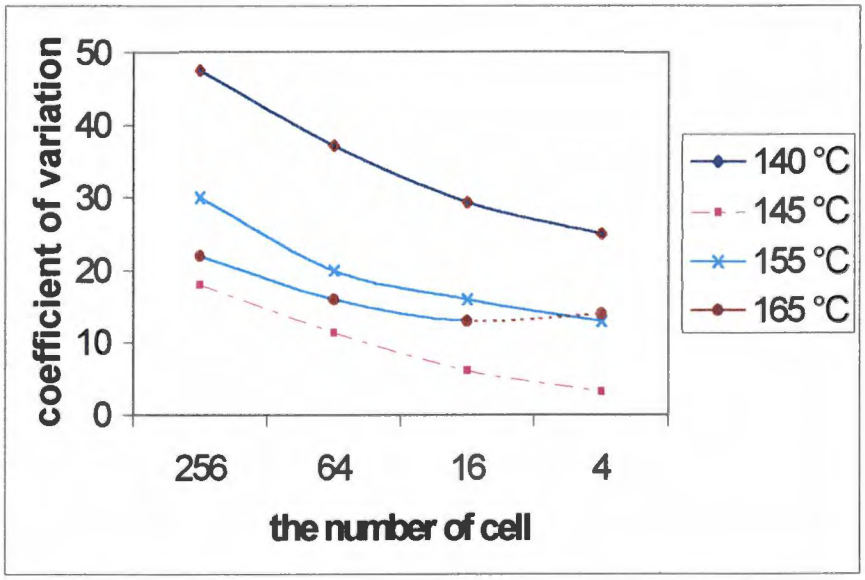

Figure 4-13. Coefficient of variation spectra of glass fiber distribution of the tubes made under different mandrel temperatures

The effect of wetting die temperature

Figure 4-14 shows the load-displacement curve for two samples made under different wetting die temperatures of 180 and 210°C(shown in table 4-3). Figure 4-15 shows the comparison of the energy absorbed by these two different samples. It can be observed that as the wetting die temperature increased, similar behavior was found as for increased mandrel temperature. The displacement and the absorbed energy of the sample was increased tremendously.

Table 4-3 The study for wetting die temperature's effect on mechanical property of the tube filled with cement

No	7	8
Wetting die temperature (°C)	**180**	**210**
Mandrel temperature (°C)	155	
Mandrel speed (RPM)	10	
Wetting die speed (RPM)	30	
Exit gate pressure (bar)	2	
Usage of pre-open device	Yes	

The effect of exit gate pressure

Figure 4-16 shows the difference of the energy absorbed between two different samples made under two exit gate pressures (shown in table 4-4) The possible explanation may be that the high exit pressure will increase the breakage of the glass fiber, so the mechanical property would be harmed.

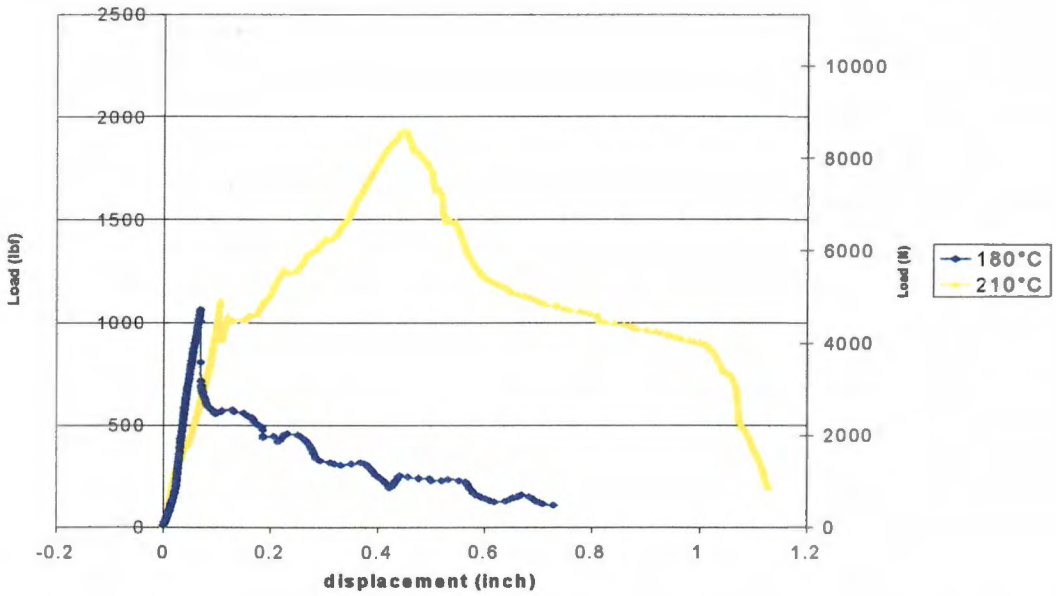

Figure 4-14. The load vs. displacement for two tubes filled with cement made under two different wetting die temperatures

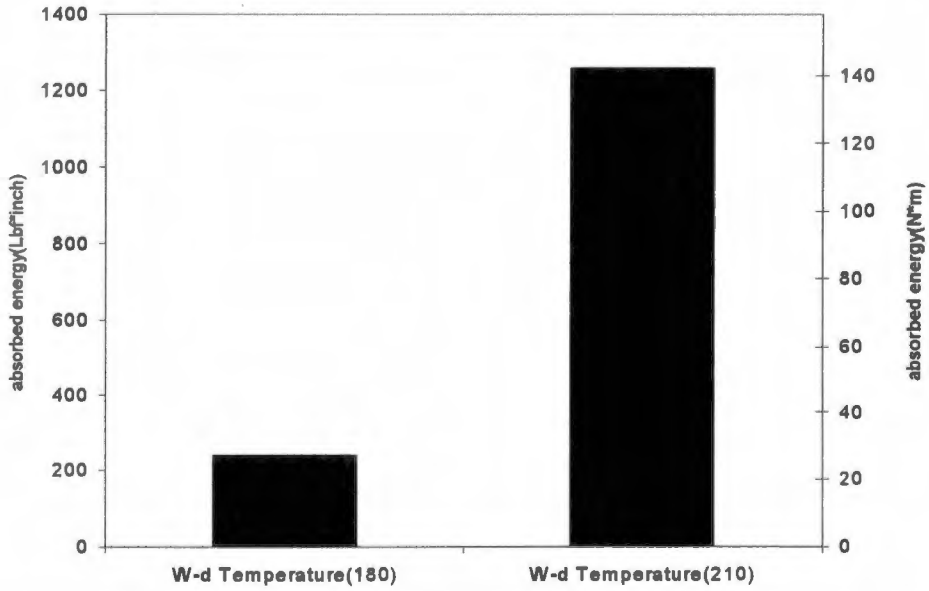

Figure 4-15. The absorbed energy of two tubes filled with cement made at two different wetting die temperatures

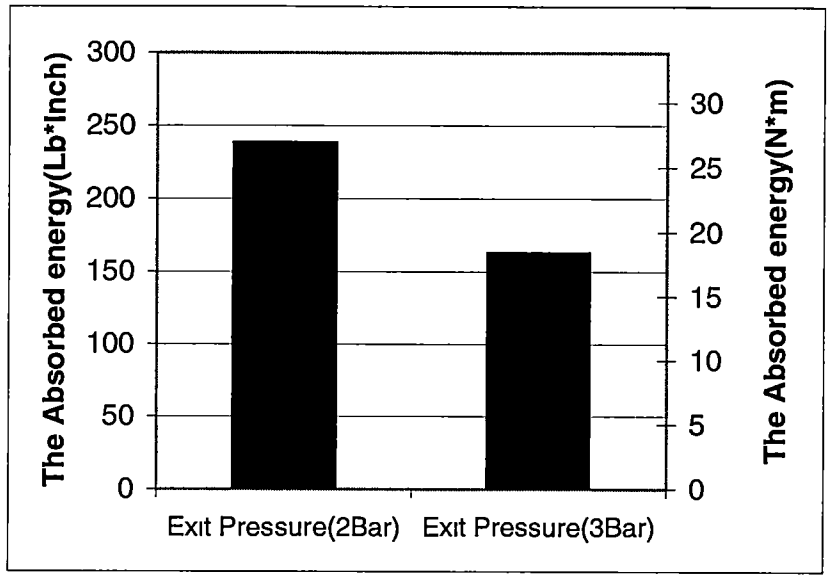

Figure 4-16 The absorbed energy of two tubes filled with cement using two different exit pressures

Table 4-4. The Study of exit gate pressure effect on mechanical property of the tube filled with cement

No	9	10
Exit gate pressure (bar)	**2**	**3**
Wetting die temperature (°C)	180	
Mandrel Temperature (°C)	155	
Mandrel speed (RPM)	10	
Wetting die speed (RPM)	30	
Usage of pre-open device	Yes	

The effect of the usage of the pre-open device

Two kind of samples were made under the conditions shown in Table 4-5. Figure 4-17 shows the usage of the pre-open device can increase the energy absorbed by the sample during the three point bending test. The pre-open device can increase the wetting between the glass fiber and the polypropylene melt by untwisting the glass fiber bundle and lower the adhesion between the glass fiber before it comes into the wetting die.

Table 4-5. The study for effect of the usage of the pre-open device on mechanical properties of the tube filled with cement

No.	11	12
Usage of pre-open device	**Yes**	**No**
Wetting die temperature(°C)	180	
Mandrel Temperature(°C)	155	
Mandrel speed(RPM)	10	
Wetting die speed(RPM)	30	
Exit gate pressure(bar)	2	

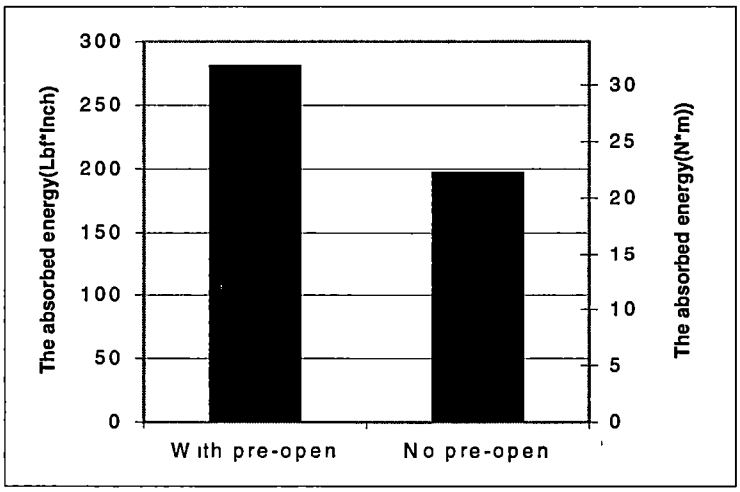

Figure 4-17 The absorbed energy of two tubes filled with cement made With pre-open device and without pre-open device

The effect of the wetting die's rotating speed

Four samples were made under the conditions shown in Table 4-6. Figure 4-18 presents the absorbed energy by the tube processed at four different wetting die rotating speed. As we can see, as the wetting die's rotating speed increases, the energy absorbed by the tube increased. A possible explanation is as the wetting die rotates faster and faster, the viscosity of the polypropylene within the wetting die would be lowered by the shear force exerted by the wetting die, so it becomes easier for the wetting die to squeeze the polypropylene melt into the glass fiber bundle and increase the wetting between the glass fiber and the polypropylene Figure 4-19 confirmed that the void content decrease as the wetting die rotating speed increases.

Table 4-6. The study for effect of different wetting die speed on mechanical properties of the tube filled with cement

No	13	14	15	16
Wetting die speed(RPM)	**0**	**15**	**30**	**60**
Wetting die temperature(°C)	180			
Mandrel Temperature(°C)	155			
Mandrel speed(RPM)	10			
Usage of pre-open device	Yes			
Exit gate pressure(bar)	2			

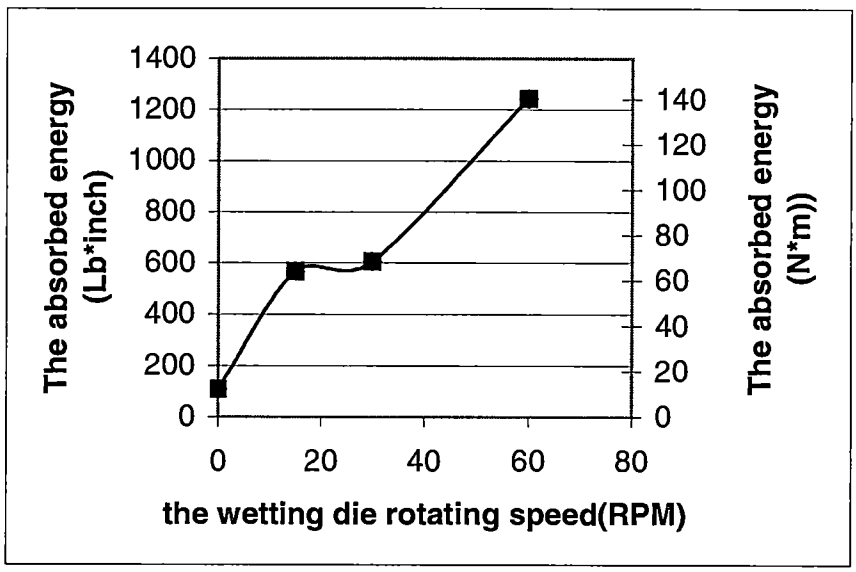

Figure 4-18. The absorbed energy of the tubes filled with cement mixture made under different wetting die rotating speeds

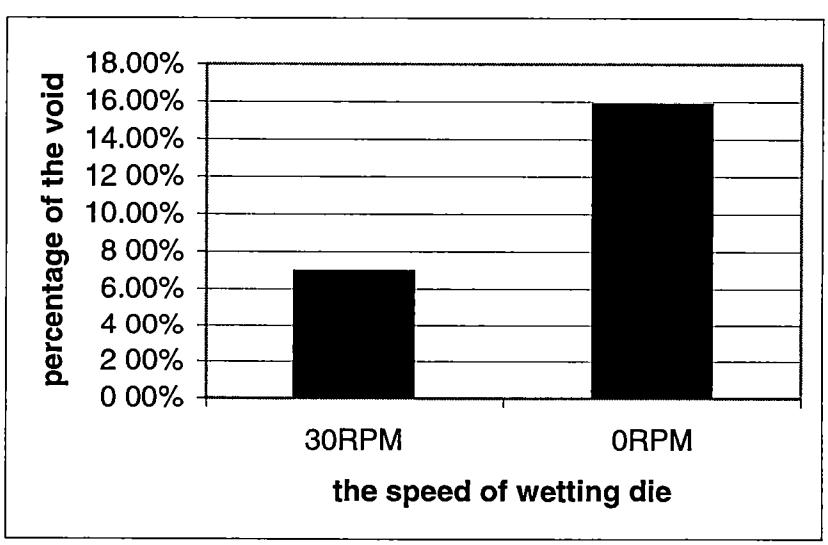

Figure 4-19. The void content of tubes made under different wetting die rotating speeds

The reinforcement of cement filled tube by internally placed PP/fiberglass tape

The tube that was reinforced by 15 internal tapes and were filled with a cement mixture was tested under three point bending. The tube was made under the condition shown in Table 4-7 and they have a fuzzy inner surface. The fundamental load deformation curve for such a specimen is shown in Figure 4-20 The table 4-8 summarizes test results and shows details of sample's mechanical characters. The calculation for the table 4-7 followed the equation (3)-(6). For purpose of this discussion the stress was taken to be the tensile component from the applied load In the figure 4-20 the structure demonstrates a very large elastic region extending perhaps to a displacement of 0 62 inches (15 24mm) over 6 inch (152.4mm) span. The maximum stress reaches to 10.3 ksi when strain is 0 22. After the maximum stress was reached, the structure didn't fail suddenly, but undergo progressive damage while maintaining some load carrying capacity. The stress of the plateau part the curve in figure 4-20 is around 2.6 ksi (17.9Mpa) The structure didn't fail until the strain reach to 0 41. The stress at failure is 1.8 ksi (12 4MPa). This non-suddenly-fail property would be important within areas like San Francisco where earthquakes are frequent.

Table 4-7 The processing factors of the tube used of internal tape reinforced

No	17
Usage of pre-open device	yes
Wetting die temperature(°C)	210
Mandrel Temperature(°C)	165
Mandrel speed(RPM)	10
Wetting die speed(RPM)	30
Exit gate pressure(bar)	2

Table 4-8. The Mechanical property of the tube reinforced with internally tapes

Modulus	Maximum Stress	Strain at Maximum Stress	Stress at failure	Strain at failure
100 ksi 689 4MPa	10.3 ksi 71MPa	0.22	1.8 ksi 12 4Mpa	0.41

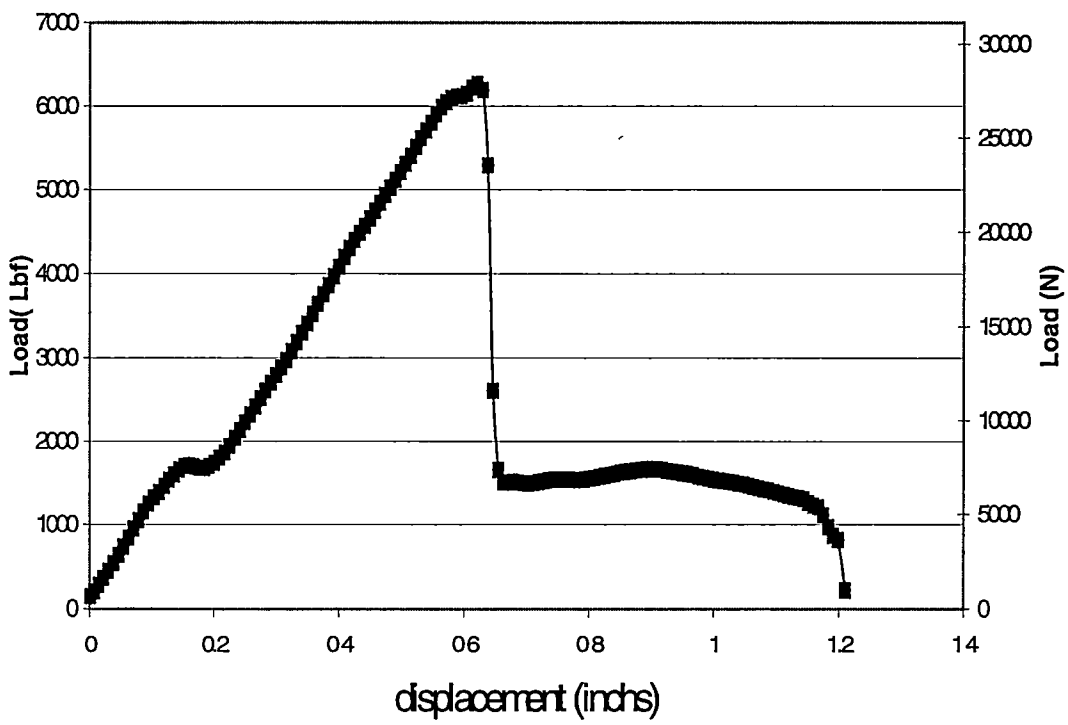

Figure 20 The load vs displacement curve of the tube filled with cement mixture and with 15 internal tapes

The fatigue test

The processing factors of tubes, whose fatigue properties were tested in continuous three point bending, are shown in Table 4-9.

The tubes made under higher mandrel temperature have a fuzzy inner surface, and the tube made under lower mandrel temperature has a smooth inner surface. From the Figures 4-21 and 4-22 the elastic behavior of the tubes filled with cement and internal tapes were observed. Each specimen's modulus did not change much until failure occures, and the sample's displacement would recover when the load was released beforce the sample's failure.

A huge difference of the fatigue life between the tube with smooth inner surface and the tube with fuzzy inner surface was found. Under about 50% of the maximum load that they can take, the fatigue life of the tube with fuzzy inner surface is about twice as that of the tube with smooth inner surface This shows the fuzzy surface contribute a substantial advantage of the improving the tubes' fatigue properties over those of tubes with smooth surface.

Table 4-9. The processing factors used to make tubes to be reinforced with internal tapes

No	18	19
Mandrel temperature (°C)	140	165
Usage of pre-open device	yes	
Wetting die temperature (°C)	210	
Mandrel speed (RPM)	10	
Wetting die speed (RPM)	30	
Exit gate pressure (bar)	2	
Internal tapes	15	

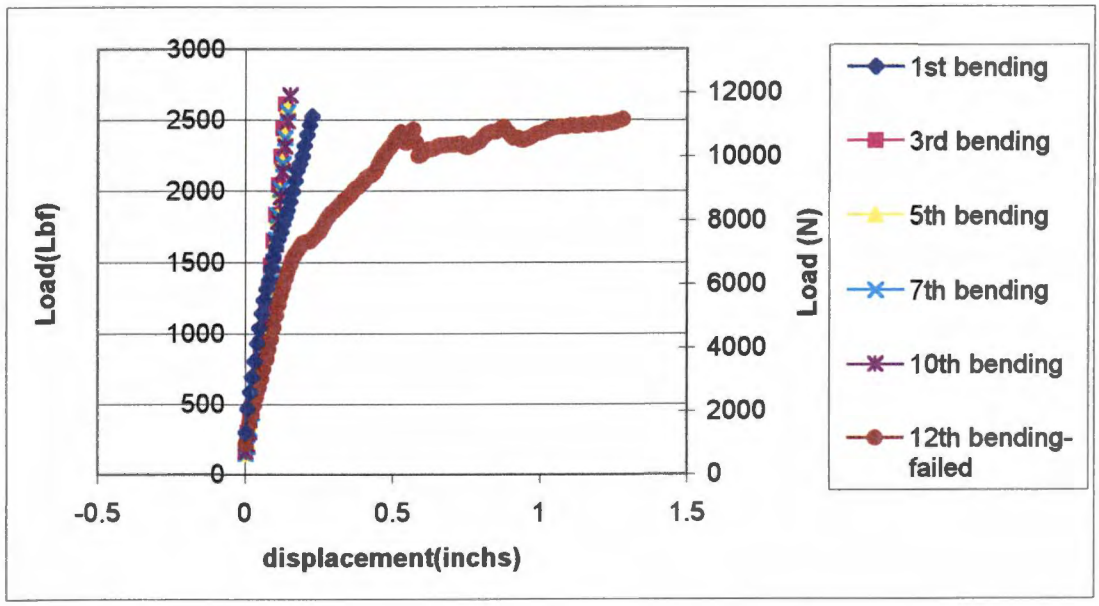

Figure 4-21. The load vs. displacement curves of the tubes with smooth inner surface filled with cement mixture and reinforced with 15 internal tapes (samples failed after 12 times of bending)

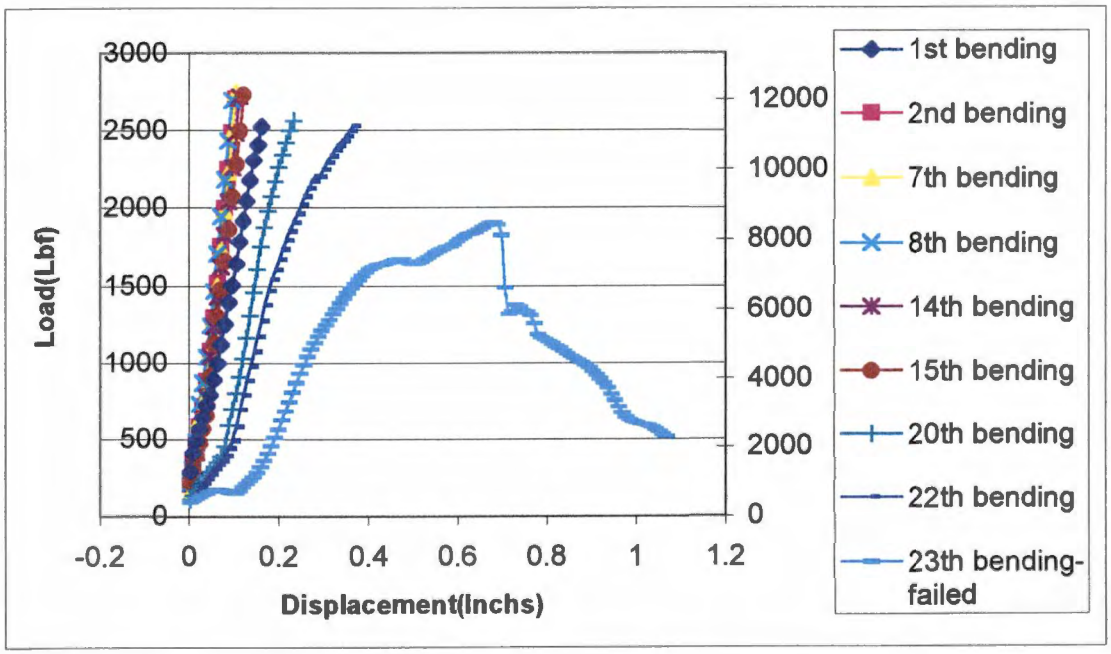

Figure 4-22. The load vs. displacement curves of the tubes with fuzzy inner surface filled with cement mixture and reinforced with 15 internal tapes (samples failed after 23 times of bending)

Conclusions

- This composite has good potential to provide superior reinforcement in cement or concrete structures. Reinforced with 15 internal tapes, the maximum tensile stress of the tube filled with a cement mixture reaches an astonishing 10.3 ksi (71 MPa). And after maximum stress was reached, the structure will not fail until the strain get to 0 41 and maintain a stress around 2 6 ksi (17.9 MPa).
- The temperature of mandrel and wetting die has a very strong effect on the composite's mechanical properties With the operational range from 140°C to 165 °C, increasing temperature can diminish the void content within the composite and produces a unique "fuzzy" inner surface for the cylinder.
- The appropriate choice of rotation rate for the wetting die, the usage of the pre-open device and appropriate exit gate pressure can help the composite improve its mechanical properties.
- The development of a unique "fuzzy" inner surface of the tube has the ability to improve the strength and fatigue properties of the composite
- To further compare and analyze the material properties found in these composites, Table 5-1 shows the available data to compare the stress among the steel, concrete, thermosetting rebar, steel reinforced concrete, and the internal tapes reinforced tubes investigated in this project. It was found that the maximum stress of the tube reinforced with internal tapes are two times of that of the steel

reinforced concrete and that the tube reinforced with internal tapes can stand hundred to more than thousands times strain than other materials

Table 5-1. The comparison among tensile property of different materials

Materials	maximum tensile stress	Strain at maximum tensile stress
concrete	1.4-4.1 MPa 200-600 psi	1×10^{-5}
Steel bar	379-861MPa 55-100 ksi	0 002-0.0035
Pultruded thermosetting GF rebar	600 MPa(typical value) 87.03 ksi	0 015
Steel reinforced concrete	16.8-31.7MPa* 2.4-4.6 ksi	0.0005-0.0009*
Internal tapes reinforced tube	71 MPa** 10.3 ksi	0.22**

* These values are got based on the lamellar composite model when a uniaxal load is applied paralled with the layers, the maximum reinforcement of steel rebar volume ratio is 0 04

** The reinforcement of internal tapes volume ratio is 0.04

BIBLIOGRAPHY

[1], C Bedard, Concrete International, **14,** 55 (1992).

[2] M. Fickelhorn, Materials and Structure Jounal, **23**, 317 (1990).

[3] H. M. Makhtouf, B. H. Ahmadi, and J. Al-Jabal, "Concrete International, **13** 65 (1991).

[4] K.M. Howell, Materials Performance, **12,** 15 (1990).

[5] S R Yeomans, Corresion, **50**, 72 (1994)

[6] A. Nanni, and C. Dolan, Proc., Fiber-Reinforced-Plastic Reinforcement for Concrete structure, American Concrete Institute, Detroit, Mich., 766 (1993).

[7] D.I. Kachlakev, and J R. Lundy, Proc., 4th Mat. Conf.: Materilas of the New Millennium, ASCE, Reston, Va., 638, (1995).

[8] F N. cogswell , Inst Phys Conf. Ser. **89** 77 (1988)

[9] M Hou, L. Ye, and Y. W Mai, Plastic, Rubber and Composites Processing and applications, **23,** 279 (1995)

[10] J. D. Muzzy, A O Kays, Polymer Composites **5,** 169 (1984).

[11] R. Marissen, H H. Hornman, and L.E.P. Wenmakers, Plastic-Metals- Cermics **18** 41, (1990).

[12] Z.J. Bor, Advanced polymer composites: Priciples and Application, ASM Metals Park, Ohio (1994).

[13] K. K Chawla, Composite Materials, Springer-Verlag, New York 1987

[14] P R, Scott; T. Thanasis; Proc, First Int Conf High Speed Ground Transp Syst., ASCE, New York, Ny, USA, 522 (1993).

[15] J C. Philp, Civil Enfineering, **69,** 65 (1999).

[16] E. J. Rabun, M H Edward, PCI-J, **36** 26 (1991).

[17] L. Howard, S. K. Edward, PCI-J **41**, 14 (1996).

[18] V. L. Brown, C. Bartholomew, ACI Materils Journal. **90**, 34 (1993).

[19] J. Larralde, R.Silva, Journal of Testing and Evaluation. **22** 351 (1994).

[20] H. Saadatmanesh, R.M. Ehsani, Proc., Structure Congress, Structural Materials, J. F. Orifino, Ed., ASCE, New York, 526 (1989).

[21] J. Larralde, L. Renbaum, Proc, Structures Congress, Structural Materials, J. F. Orofino Ed., ASCE, New York, 261 (1989).

[22] B. Benmokrane, B. Tighiouart,, ACI Materials Journal, **93**, 246 (1996) .

[23] L Malvar, ACI Materials Journal, **92,** 276(1995).

[24] M,R. Ehsanı, H. Saadatmanesh,, ACI Materials Journal, **92**, 391 (1995)

[25] A Braimah, M F. Green, Journal of Composite for construction **2**, 149 (1998).

[26] C. R Michaluk, S. H. Rizkalla, ACI Structural Journal, **95,** 353(1998).

[27] S.V Kumar, R H Ganga, Journal of Structural Engineering, **124**, 11(1998).

[28] R Adimı, B. Benmokrane; Structure Composite Materials, Structural Systems, Telecommunication Towers Proceedıng, Annual Co, Canadian Soc for Civil Engineering, Montreal, Que, Can **6,** 121 (1997).

[29] S.S Faza, H.V.S. Gangarao, TRB 70th Annual Meeting, Paper No. 91-0638 (1991)

[30] NEFCOM Corporation, NEFMAV-Technical Leaflet 1, New Fiber Composite Material for Reinforcing Concrete, Tokyo, Japan, (1988)

[31] E. R Schmeckpeper, R. Nielsen; Structures Congress XII Pro.c Struct Congr 94, ASCE, New York, NY USA, 1250 (1994)

[32] N Banthia,; C. Yan,; ACI Materials Journal; **95,** 11 (1998).

[33] G. A. Sulaimanı, A. Sharif, ACI Structural Journal, **91**, 283(1994).

[34] M. Saadatmanesh, M.R. Ehsanı, Concrete International, **12**, 65 (1990).

[35] A. Sharif, G. A. Sulaimani, ACI Structural Journal, **91**, 189 (1994).

[36] A.Mirmiran, M. Shahawy; Composıtes Part B. Enginee ring. Proceeding of 1995 2nd Internatial conference For composite engineering New Orleans, LA, USA **27** 263(1996)

[37] S Aberdeen, Concrete Construction, **35**, 508 (1990).

[38] L. Moore, Plant Engineering, **42**, 74 (1998).

[39] H Saadatmanesh, M R Ehsani, ACI Construction Journal, **91**, 434 (1994).

[40] Y Q Lu, D.J Kennedy, Canadıan Society for Civil Engineering **21,** 111(1992)

[41] Y H Chai M J.N Priestley, Proc. 2rd Brıdge Engineering. Conference, Denver, **1290**, 95 (1991)

[42] M J.N .Prıestly, R. Park, ACI Structural Journal, **84,** 61(1987).

[43] M.J N Priestly, F Seıble, Proc. of Advanced Composite Materials in Brideges and Structure, Canandian Society for Cıvil Engineering, 287 (1992).

[44] H Saadatmanesh, M R Ehsani, ACI Structural Journal, **93,** 639 (1996).

[45] Shah, S. P. Ludirdja, D.; ACI Materials Kournal, v 85 Sept /Oct. 1988 p 352-360

[46] E. A. McDougle, Constructıon Specıfier. **48** 46 (1995).

[47] B.A. Proctor, Glass-Current Issue. Edıted by A.F. Wright and Jupuy. Martınus Nijhiff, Dordrecht, Neterhland, , 555 (1985)

[48] A Bentur, M B. Bassat; Journal of American Ceramic Society, **68**, 203 (1985).

[49] B. Steffestun, G. H Frischat, Journal of American Ceramic Society, **76**, 699, (1993)

[50] Y Hu, J Cheng, Glass Technology, **39** 204 (1998)

[51] C. M. Huang, D. Zhu, Journal of the American Ceramic Society. **80,** 2326 (1997)

[52] J. P. Broomfield, "Corrosion of steel in concrete" London; New York: E&FN Spon, (1997)

[53] "Corrosion forms and control for infrastructure" Philadelphia, PA: ASTM, (1992)

[54] P.A Schweitzer, " What every engineer should know about corrosion,: Marcel Sekker Inc. New York and Basel (1985)

[55] I. Soroka, "Portland cement paste and concrete" London : Macmillan, (1979).

[56] F R.Shanley, "Strength of materials" New York, McGraw-Hill, (1957).

[57] PPG Industries, shelby N.C.

[58] H. Meng, Y. Lin, Plastic, Rubber and Composites Processing and applications **23** 279 (1995).

[59] J. D Muzzy, A. O Kays, Polymer Composites **5,** 69 (1984).

[60] R. Marissen, H.H. Hornman,, and L.E.P Wenmakers,. Plastic-Metals- Cermics 41(1990)

[61] K K.Chawla, Composite Materials, Springer-Verlag, New York 1987.

[62] C. M. Susan and S. S George.; Journal of Composite Materials, **26**, 2348 (1992)

[63] F P. Beer, E.R Johonston, Mechanics of materials, Mcgraw-Hill, New york 1992

[64] R E. swain, K.L. Reifnider, K. Jayaraman. And m Elzein, J. thermoplastic Compos. Mater., **3**, 13 (1990).

[65] J. Delmonte, Technology of carbon and Graphite Composites, Van Nostrand Reinholdt Co. (1980).

[66] J.T. Harness, SPE NATEC Pro., Bal Harbour , FL, Oct, (1982)

[67] D F. Adams and D.R. Doner, J. compos. Mater., **1**, 4 (1967)

[68] R.S. Zimmerman and D.F. Adams, NASA CR_177970, (1985).

[69] M. N. Ghasemi , R.D. Cope; S I Guceri; Transactions of ASME , **113**, 304 (1991)

[70] F K. SmithMat, Tech **11**101 (1996).

[71] H. Joachim, K. L. Sang, and K. V. Steiner 36th International SAMPE symposium 2142 (1991).

[72] Jay Randall Sayre, master thesis " The effect of bias angle and fiber volume fraction on the mechanical properties if filament-wound polyproplene-galss tubes, Master thesis, University of Tennessee, Knoxville (1997)

[73] M L.Enders, proc. 22nd international SAMPE Technical Conference 88(1990)

[74] R.M. Jones, Mechanics OF Composite materials, Scripta Book Company, New York (1975)

[75] R R. Bresee, Daniluk, Tappi Journal **80** 133 (1997)

[76] L. E P. Wenmaker, A. E. Galman, R Marissen.; Proc. Internat. Symp. 'Advanced materials for lightweight structures ' ESTEC. Noordwijl, The Netherland 197 (1992).

[77] H. Hiroyuki, Z. I. Maekawa., N. Ikegawa and T. Matsuo ; Polymer Composites, **14**, 308 (1993)

[78] R. Juran,.; Modern Plastic Encyclopedia, McGraw-Hill, New York (1991)

VITA

Yuanheng Zhang was born in Henan Province, P. R. China, on March 08,1973. He joined Zhengzhou Univeristy in September 1990 and received his Bachelor of Materials Engineering Degree in July 1994. He continued his study in Beijing University of Chemical Technology and achieved the Master Degree in polymer engineering in 1997. In August 1997 he joined the Ph.D's program in Material Science and Engineering department at the University of Tennessee, Knoxville, and transfer to master's program in 1999 He received his degree in December 2000. He was employed as Graduate Research Assistant and Graduate Teaching Assistant in the department of Materials Science and Engineering during his stay at the University of Tennessee His research interests are in polymer processing and characterization.